SOLAR DRIVEN MEMBRANE DISTILLATION UNIT

A Final Year Project Report

Presented to

SCHOOL OF MECHANICAL & MANUFACTURING ENGINEERING

Department of Mechanical Engineering

NUST

ISLAMABAD, PAKISTAN

In Partial Fulfillment

Of the Requirements for the Degree of

Bachelors of Mechanical Engineering

By

Anas Imdad

Israr Ahmed

Abdullah Tofique

June 2018

EXAMINATION COMMITTEE

We hereby recommend that the final year project report prepared under our supervision by:

ANAS IMDAD	NUST201433027
ISRAR AHMED	NUST201432086
ABDULLAH TOFIQUE	NUST201432980

Titled: "**SOLAR DRIVEN MEMBRANE DISTILLATION UNIT**" be accepted in partial fulfillment of the requirements for the award of **MECHANICAL ENGINEERING** degree.

Supervisor: **Dr. Zaib Ali** _____

Dated:

Committee Member: **Dr. Emad ud Din** _____

Dated:

Committee Member: **Dr. Muhammad Sajid** _____

Dated:

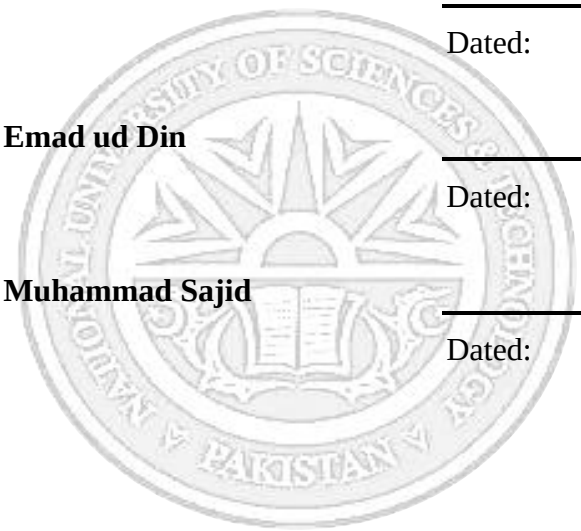

_____ _____

(Head of Department) (Date)

COUNTERSIGNED

Dated: _____ _____

(Dean / Principal)

ABSTRACT

Solar powered distillation is an attractive method for producing clean water in remote areas. The basic objective of this work is to prepare a small scale standalone system for the production of fresh water. A closed loop distillation system based on direct contact membrane distillation (DCMD) is developed and then it is integrated with solar collector. All the energy requirements for the system are met by solar collector. A mathematical model is developed which is dependent on heat and mass transfer within the DCMD module in order to predict the effectiveness of the system under different working parameters. Poiseuille and Knudsen model is used for this purpose which is then solved using MATLAB® software numerically. The verification of model is done by means of parametric analysis. This proposed model is then used to figure out the temperature difference across the both surfaces of hydrophobic membrane which then led to the calculation of pressure difference across the membrane which then led to the result of permeate flux. The results of mathematical model are then verified through simulations by using COMSOL® software and the optimum working conditions for the system are identified. Also the modelling of solar collector is done to evaluate the temperature of fluid after the process of heating from Sun. This also became the basis of MATLAB® code which demanded evaluation of versatile coefficients for various reasons. A small scale working prototype is also developed in order to validate the theoretical results. From experimentation, it is observed that the water flux increases with increasing the bulk feed temperature, bulk feed velocity, porosity of membrane and decreases with increasing the bulk permeate temperature, decreasing the bulk permeate velocity, increasing the membrane thickness etc.

PREFACE

Clean drinking water is one of the basic necessities of life. It is a major global problem and according to present experts, next world war will be based on the sources of clean water. 780 million people in the world lacks clean drinking water and by 2025, an estimated 1.8 billion people will live in areas plagued by water scarcity, with two-thirds of the world population living in water stressed regions. Talking about our country, Pakistan is at the 17th position in the world which are facing water crisis. Our project is based on solving this problem (by using only sunlight as energy source) economically and efficiently by a technique named as direct contact membrane distillation.

Keeping in mind the energy crisis in Pakistan, this is indeed one of the best methods devised so far for the production of clean drinking water by solar energy. This technique is very efficient and economical as it removes nearly 99% of the salts from the sea water by using merely sunlight.

Proper waste water treatment is another arising issue in developing urban areas which can be addressed by the method we worked on in a very economical way. This unit can be used not only for the production of drinking water in areas near sea but also for the treatment of chemically polluted and hazardous waste water produced from the industries in very cost effective way. These small portable standalone units can easily produce enough water to fulfill the requirements of a house by putting it simply on the roofs even in hilly areas where lack of drinking water is a major issue now a days.

We worked on making the method more efficient and cost effective by making a standalone unit, using solar energy only as the external source of energy.

ACKNOWLEDGMENTS

First of all, Thanks to Almighty Allah who gave us the strength, courage and required skills to complete all the tasks successfully, without His help we would not have been able to take the project to the pinnacle of success indeed. We are blessed and thankful to our parents who motivated and guided us at every step to achieve our goals.

We are highly indebted to our project supervisor Dr. Zaib Ali for his continuous guidance, encouragement and technical insight throughout the project. We are extremely grateful to Hafiz M. Abd-ur-Rehman who helped and facilitated us in the mathematical modeling of the solar panel of our project. We are also thankful to our senior Mujahid Saeed and our batch mate Ahmed Rizvi for his suggestions and ideas regarding the fabrication of our prototype.

We would like to appreciate the guidance given by panels especially in our project presentation that has improved our presentation skills thanks to their comment and advices. However, it would not have been possible without the kind support and help of many individuals and organizations. I would like to extend my sincere thanks to all of them.

Last but not the least, we would like to thank our university “National University of Sciences and Technology (NUST)”, specifically the department of Mechanical and Manufacturing Engineering (SMME) and Institute of Environmental Sciences and Engineering (IESE) for their cooperation

ORIGINALITY REPORT

We hereby declare that no portion of the work of this project or report is a work of plagiarism and the workings and findings have been originally produced. The project has been done under the supervision and guidance of Dr. Zaib Ali and has not been a support project of any similar work serving towards a similar degree's requirement from any institute. Any reference used in the project has been clearly cited and we take sheer responsibility if found otherwise.

PLAGAIRISM CHECK

ORIGINALITY REPORT

10%	6%	6%	1%
SIMILARITY INDEX	INTERNET SOURCES	PUBLICATIONS	STUDENT PAPERS

PRIMARY SOURCES

1	opus.ipfw.edu Internet Source	3%
2	Khalifa, A., H. Ahmad, M. Antar, T Laoui, and M. Khayet. "Experimental and theoretical investigations on water desalination using direct contact membrane distillation", Desalination, 2017. Publication	2%
3	Parimal Pal. "Arsenic Removal by Membrane Distillation", Elsevier BV, 2015 Publication	1%
4	Submitted to Imperial College of Science, Technology and Medicine Student Paper	<1%
5	Kharton, Vladislav V., Alexandre P. Viskup, Eugene N. Naumovich, and Fernando M. B. Marques. "Oxygen ion transport in La2NiO4â€ based ceramics", Journal of Materials Chemistry, 1999. Publication	<1%
6	www.pdacom.net Internet Source	<1%
7	researchbank.rmit.edu.au Internet Source	<1%
8	www.mattglattfelder.com Internet Source	<1%
9	Saleh, Ahmad M., Hosni I. Abu-Mulaweh, and Donald W. Mueller. "Flat-Plate Solar Collector in Transient Operation: Modeling and Measurements", Volume 8B Heat Transfer and Thermal Engineering, 2013. Publication	<1%
10	Rao, Guiying, Sage R. Hiibel, Andrea Achilli, and Amy E. Childress. "Factors contributing to flux improvement in vacuum-enhanced direct contact membrane distillation", Desalination, 2015. Publication	<1%
11	Khayet, M.. "Monte Carlo simulation and experimental heat and mass transfer in direct contact membrane distillation", International Journal of Heat and Mass Transfer, 201003 Publication	<1%
12	kth.diva-portal.org Internet Source	<1%
13	Sofiane Soukane, Mohamed W. Naceur, Lijo Francis, Ahmad Alsaadi, Noreddine Ghaffour. "Effect of feed flow pattern on the distribution of permeate fluxes in desalination by direct contact membrane distillation", Desalination, 2017 Publication	<1%
14	Daniel González, José Amigo, Francisco Suárez. "Membrane distillation: Perspectives for sustainable and improved desalination", Renewable and Sustainable Energy Reviews, 2017 Publication	<1%
15	Srisurichan, S.. "Mass transfer mechanisms and transport resistances in direct contact membrane distillation process", Journal of Membrane Science, 20060601 Publication	<1%
16	Khayet, M.. "Membranes and theoretical modeling of membrane distillation: A review", Advances in Colloid and Interface Science, 20110511 Publication	<1%
17	Belessiotis, Vassilis, Soteris Kalogirou, and Emmy Delyannis. "Membrane Distillation", Thermal Solar Desalination, 2016.	<1%

18	mdpi.com Internet Source	<1%
19	www.cheng.cam.ac.uk Internet Source	<1%
20	Submitted to National University of Ireland, Galway Student Paper	<1%
21	www.tssdjx.com Internet Source	<1%
22	Submitted to Cranfield University Student Paper	<1%
23	Ghadiri, Mehdi, Safoora Fakhri, and Saeed Shirazian. "Modeling and CFD Simulation of Water Desalination Using Nanoporous Membrane Contactors", Industrial & Engineering Chemistry Research, 2013. Publication	<1%
24	Submitted to Swansea Metropolitan University Student Paper	<1%
25	Submitted to Nanyang Technological University, Singapore Student Paper	<1%
26	Cavenati, S.. "Separation of CH"4/CO"2/N"2 mixtures by layered pressure swing adsorption for upgrade of natural gas", Chemical Engineering Science, 200606 Publication	<1%
27	Boukhriss, Mokhless, Khalifa Zhani, and Habib Ben Bacha. "Optimization of membrane distillation (MD) technology for specific application desalination", The International Journal of Advanced Manufacturing Technology, 2016. Publication	<1%
28	Rohit Ruhal. "Membrane Separation and Design", Handbook of Food Process Design Ahmed/Handbook of Food Process Design, 03/21/2012 Publication	<1%
29	S. E. Labance, , P. H. Heinemann, R. E. Graves, and D. M. Beyer. "EVALUATION OF THE EFFECTS OF FORCED AERATION DURING PHASE I MUSHROOM SUBSTRATE PREPARATION: PART 1. MODEL DEVELOPMENT", Transactions of the ASABE, 2006. Publication	<1%
30	Ashoor, B.B., S. Mansour, A. Giwa, V. Dufour, and S.W. Hasan. "Principles and applications of direct contact membrane distillation (DCMD): A comprehensive review", Desalination, 2016. Publication	<1%
31	Li, Yanxia, Zhongliang Liu, and Liang Feng. "Effect of Physical Parameters on Thermal Behavior of Microcombustor", Journal of Thermophysics and Heat Transfer, 2012. Publication	<1%
32	core.ac.uk Internet Source	<1%
33	Adnan, S.. "Commercial PTFE membranes for membrane distillation application: Effect of microstructure and support material", Desalination, 20120104 Publication	<1%
34	ediss.uni-goettingen.de Internet Source	<1%
35	d-nb.info Internet Source	<1%
36	Kiani, K.. "Free vibration of in-plane-aligned membranes of single-walled carbon nanotubes in the presence of in-plane-unidirectional magnetic fields", Journal of Vibration and Control, 2015. Publication	<1%
37	Rejeb, Oussama, Houcine Dhaou, and Abdelmajid Jemni. "Parameters effect analysis of a photovoltaic thermal collector: Case study for climatic conditions of Monastir, Tunisia",	<1%

38	Hawari, Alaa H., Nagla Kamal, and Ali Altaee. "Combined influence of temperature and flow rate of feeds on the performance of forward osmosis", Desalination, 2016. Publication	<1%
39	quadrant.matweb.com Internet Source	<1%
40	Upadhyaya, Sushant, Kailash Singh, S.P. Chaurasia, Rajeev Kumar Dohare, and Madhu Agarwal. "Mathematical and CFD modeling of vacuum membrane distillation for desalination", Desalination and Water Treatment, 2015. Publication	<1%
41	Kim, Jin Man, Soon Ho Kang, Dong In Yu, Hyun Sun Park, Kiyofumi Moriyama, and Moo Hwan Kim. "Smart surface in flow boiling: Spontaneous change of wettability", International Journal of Heat and Mass Transfer, 2017. Publication	<1%
42	abcm.org.br Internet Source	<1%
43	McDonald, . "Fundamentals of Heat Exchanger Design", Introduction to Thermo-Fluids	<1%
	Systems Design McDonald/Introduction to Thermo-Fluids Systems Design, 2012. Publication	
44	Green Energy and Technology, 2009. Publication	<1%
45	Bhattarai, S.. "Simulation and model validation of sheet and tube type photovoltaic thermal solar system and conventional solar collecting system in transient states", Solar Energy Materials and Solar Cells, 201208 Publication	<1%
46	Hua Wang. "Experiment and Numerical Simulation of a Seawater Solar Pond", Challenges of Power Engineering and Environment, 2007	<1%
47	Alkhudhiri, A.. "Membrane distillation: A comprehensive review", Desalination, 20120215 Publication	<1%
48	Majumder, Subrata Kumar. "Heat Transfer Characteristics", Hydrodynamics and Transport Processes of Inverse Bubbly Flow, 2016. Publication	<1%
49	Lee, Jung-Gil, Eui-Jong Lee, Sanghyun Jeong, Jiaxin Guo, Alicia Kyoungjin An, Hong Guo, Joonha Kim, TorOve Leiknes, and Noreddine	<1%
	Ghaffour. "Theoretical modeling and experimental validation of transport and separation properties of carbon nanotube electrospun membrane distillation", Journal of Membrane Science, 2016. Publication	
50	math.usask.ca Internet Source	<1%
51	Mitchell, K.L.. "Coupled conduit flow and shape in explosive volcanic eruptions", Journal of Volcanology and Geothermal Research, 20050501 Publication	<1%
52	Khayet, M.. "Porous hydrophobic/hydrophilic composite membranes: Estimation of the hydrophobic-layer thickness", Journal of Membrane Science, 20051201 Publication	<1%
53	Al-Obaidani, S.. "Potential of membrane distillation in seawater desalination: Thermal efficiency, sensitivity study and cost estimation", Journal of Membrane Science, 20081001 Publication	<1%
54	Glushkov, Dmitrii O. Kuznetsov, Genii V.. "Numerical investigation of water droplets shape influence on mathematical modeling	<1%

55	Nene, Sanjay, Ganapathi Patil, and K Raghavarao. "Membrane Distillation in Food Processing", Handbook of Membrane Separations Chemical Pharmaceutical Food and Biotechnological Applications, 2008. Publication	<1%
56	Binous, Housam, Slim Kaddeche, and Ahmed Bellagi. "Solving two-dimensional chemical engineering problems using the chebyshev orthogonal collocation technique : SOLVING CHEMICAL ENGINEERING PROBLEMS", Computer Applications in Engineering Education, 2015. Publication	<1%
57	Zima, W., and P. Dziewa. "Modelling of liquid flat-plate solar collector operation in transient states", Proceedings of the Institution of Mechanical Engineers Part A Journal of Power and Energy, 2011. Publication	<1%

© Copyright by Anas Imdad, Israr Ahmed and Abdullah Tofique 2018

ALL RIGHTS RESERVED

TABLE OF CONTENTS

LIST OF TABLES

LIST OF FIGURES

ABBREVIATIONS

ACM	Aspen Custom Modeler
AGMD	Air Gap Membrane Distillation
CAD	Computer Aided Design
CFD	Computational Fluid Dynamics
CGMD	Conductive Gap Membrane Desalination
CNT	Carbon Nano Tubes
Conc.	Concentrated
CPU	Central Processing Unit
DCMD	Direct Contact Membrane Distillation
EC	European Commission
FEM	Finite Element Method
F.W.T	Feed Water Tank
GOF	Graphic Oxide Framework
GPM	Gallon Per Minute
HABs	Harmful Algae Blooms
H.F.W.T	Hot Feed Water Tank
ht	Heat Transfer
MD	Membrane Distillation
MEDESOL	Seawater Desalination by Innovative Solar-Powered Membrane Distillation System
MEDINA	Membrane based Desalination: an Integrated Approach

MEDIRAS	Membrane Distillation in Remote Areas
MEMD	Multi Effect Membrane Distillation
MS	MicroSoft
MSF	Multi Stage Flash
ODE	Ordinary Differential Equation
PCM	Phase Change Material
PDE	Partial Differential Equation
PGMD	Permeate Gap Membrane Desalination
PI	Proportional Integral
PP	Polypropylene
PTFE	PolyTetraFluoroEthylene
PV	Photo Voltaic
PVDF	Polyvinylidenefluoride
RO	Reverse Osmosis
SGMD	Sweeping Gas Membrane Distillation
SMADES	Small-scale, Stand-alone Desalination system
tds	Transport of Diluted Species
TNO	Netherlands Organization for Applied Scientific Research
TPC	Thermal Polarization Coefficient
VMD	Vacuum Membrane Distillation
V-MEMD	Vacuum- multi effect Membrane desalination

NOMENCLATURE

General:

Q	Heat flux	W m^{-2}
h	Heat transfer coefficient	W m^{-2} K^{-1}
T	Absolute temperature	K
J_w	DCMD flux	m s^{-1}
H	Enthalpy	J kg^{-1}
d_p	Mean pore size	nm
k	Thermal conductivity	W m^{-1} K^{-1}
Re	Reynolds number	
Nu	Nusselt number	
Pr	Prandl number	
d	Hydraulic diameter	m
Cp	Specific heat capacity	J kg^{-1} K^{-1}
v	Average velocity	m s^{-1}
P	Total pressure	Pa
P^v	Vapor pressure of water	Pa
p	Liquid pressure	Pa
P_a	Air pressure	Pa
B_m	Net DCMD permeability	s m^{-1}
R	Gas constant	J mol^{-1} K
K_n	Knudsen Number	

r	Mean pore radius	nm
M	Molecular weight of water	kg mol^{-1}
D	Water diffusion coefficient	m^2 s^{-1}
TPC	Temperature polarization coefficient	
EE	Evaporation efficiency	
q_t	Total heat transfer	W
i	Specific enthalpy	J/kg
L	Analyzed collector length	m
$\dot{m}$	Mass flow rate	Kg/s
d	Collector tube diameter	m
n	Total number of solar collector tubes	
V	Volume	m^3
p	Tube pitch	m
w	Velocity of fluid	m/s
M	Total number of nodes perpendicular to the direction of flow	
r	Collector tube radius	m
N	Total number of cross sections of solar collector	
z	Coordinate (Spatial)	m

Greek symbols:

τ	Tortuosity

ε	Porosity	%
ρ	Density	kg m^{-3}
δ	Total membrane thickness	μm
μ	Water dynamic viscosity	kg m^{-1} s^{-1}
λ	Mean free path	nm
ΔH_v	Latent heat of vaporization	kJ mol^{-1}
$\tau\alpha$	effective transmittance-absorption coefficient	
β	Inclination angle of solar collector	rad
α	Coefficient of Absorptivity	
σ	Stefan-Boltzmann constant	$W/(m^2K^4)$
Δz	Change in spatial coordinate	m

Superscript:

c	Combined Knudsen/ordinary diffusion	

Subscripts:

f	Feed	
b	Bulk	
m	Membrane	
$M.T.$	Mass transfer	

$conv.$	Heat transfer due to convection
$cond.$	Heat transfer due to conduction
L	Liquid phase
p	permeate
g	Gas phase
in	Inlet
out	Outlet
v	Vapor phase
ab	Absorber
i	Insulation
inn	Inner
o	Outer
am	Ambient
t	Total
g	Glass cover
c	Convection
f	Fluid circulating in the Solar collector
r	Radiation coming from S

CHAPTER 1: INTRODUCTION

1.1 Motivation

Fresh water is considered to be the lifeblood of life and it is the right of each and every person in this world to get pure and potable water. But the water crisis is a bitter dilemma and the threatening concern that exists around it is that it is not getting the deserve attention which it deserves that results in water shortage problem not for this generation only but for coming generation as well. The problem is getting even more astringent in developing countries just like Pakistan where at least 40 million people are running short of potable water. That is why according to diverse surveys, Pakistan will have insufficiency of clean drinking water by the year 2025. The problem is utterly replicated in this quote that "Water is the new oil'. This problem is further made deteriorated by Industrial sector which are polluting the lakes and rivers by industrial waste and becoming cause of further deaths. According to the UN report, about 70% of the total waste generated in the industries is being thrown into blue water [1]. There are around 250,000 children who die due to the water borne diseases and majority of these children indeed belong to the rural areas and about 840,000 die every year particularly because they don't get clean water for drinking. In addition to that, more than 80% of the diseases in the developing countries is caused by water sanitation issues [2].

So as a result of the above facts and claims, it is extremely enticing to have a cost effective desalination method or reliable process that can clean or purify the water so that remote communities can have access to this fascinating facility as demand of fresh water is rising exponentially. Around 72% of total area of Earth is covered with water and among this, around 97% of this is sea water [3]. So by employing this facility, we could eradicate this clean water problem. The proportion of the water that is clean in this world right now is only 0.8% and available in limited forms like lakes, rivers etc. but this percentage is extremely low. In response to this, presently reverse osmosis holds around 50% share of purifying the water out of other desalination methods but due to its complications and

difficulties this cannot be endorsed in Pakistan. The reasons due to which reverse osmosis cannot be used efficiently in countries like Pakistan is due to the high feed salinity of the available water bodies and the high brine concentrations that make the membranes susceptible to fouling in the RO process. Secondly, there is extremely elevated occurrence of harmful algae blooms (HABs) in the Arabian Sea, our main water source for desalination [4]. These HABs contain high concentrations of toxins that may pass through the membrane in the RO process and can cause illness on drinking and in some cases may lead to death as well.

As about 97% of total water is sea water, so this sea water could be used for the purpose of getting clean and potable drinking method by means of Membrane distillation. The outcome of the project will be clean and pure water on the other side. Furthermore, to make it more economical and cost effective, integration with natural resource like solar energy could be much more efficient and productive instead of driving it with artificial sources and energies.

1.2 Membrane distillation

Membrane desalination works on the basis of partial pressure difference on the shell and lumen side which arises due to the temperature difference. Vapors that are formed on the feed side pass through hydrophobic membrane gets condensed on the other hand and thus converted into the liquid form which is actually the clean water. Water cannot pass through membrane because membrane resists and thus blocks the water due to surface tension forces. Development of the pressure across the hydrophobic membrane also depends on the type of configuration of membrane distillation.

1.3 Background

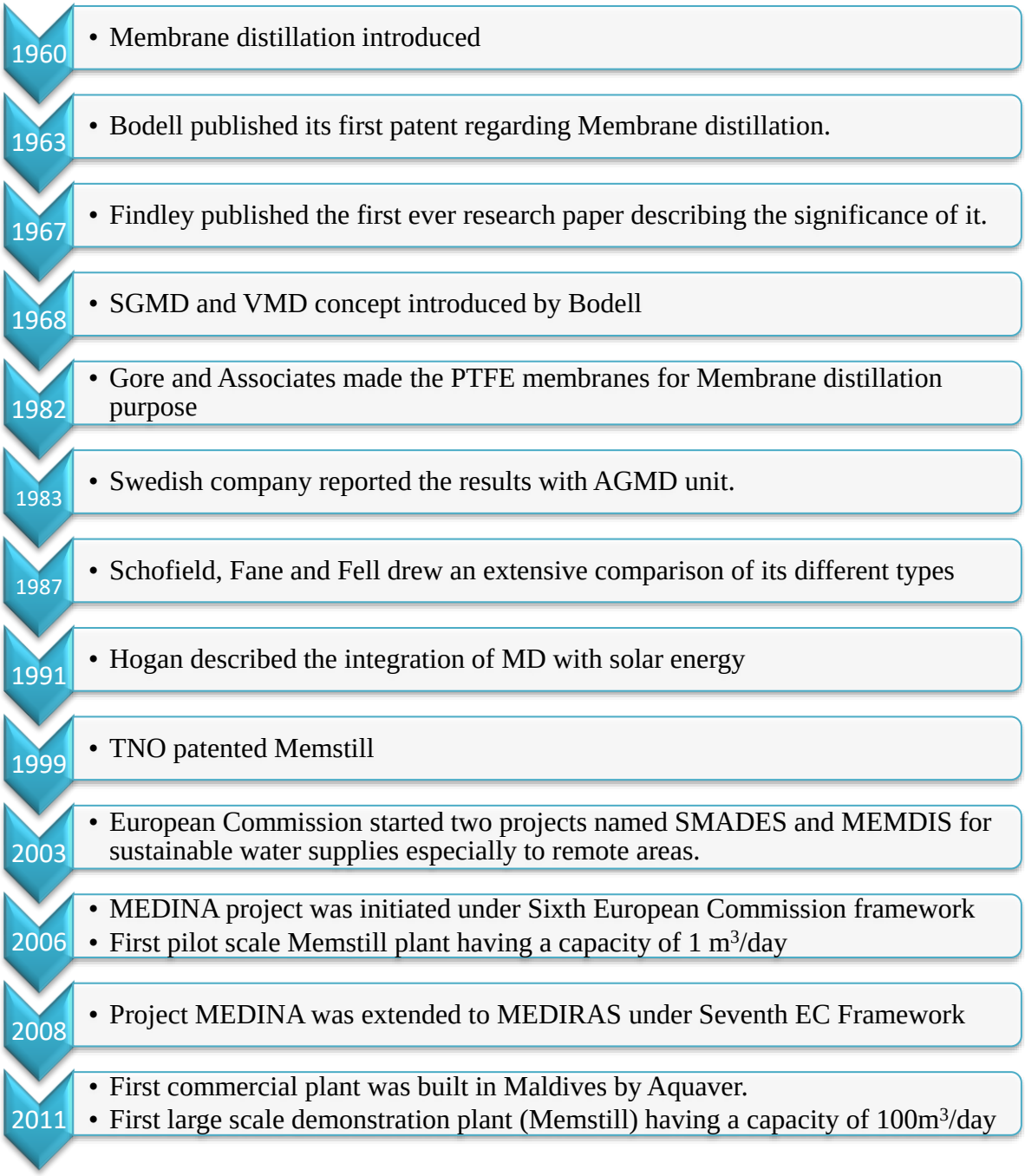

Figure 1: Chronological Background

1.4 Problem statement

To eradicate the problem of clean and pure water shortage by designing and fabricating a Membrane distillation setup incorporated with solar energy to make a "**standalone solar driven direct contact membrane distillation unit**".

1.5 Objectives of this project

- Optimum design of distillation module.
- Complete instrumentation of the module.
- Mathematical modelling of the system.
- Performing the parametric analysis and observing the trends on permeate flux in any simulation software.
- Performing the experimental comparative study by varying different parameters and recording the water flux.

1.6 Advantages

Following are the prominent advantages of MD [6].

- This membrane process can be integrated easily with other processes or natural resources like solar, wind etc.
- It can easily operate on lower temperature and pressure.
- Carrying out the separation of pure water can occur in normal conditions.
- Less stringent mechanical properties are needed for the operation.
- Characteristics of Membrane can be controlled and varied easily. So if it is used in a proper way, this could enable the access of clean water easily.
- By comparing it with other similar process for cleaning water, it is considered to be less susceptible to the limitations of flux by concentration polarization.
- More than 99% of salt rejection is achievable.

1.7 Project Plan

The tasks required for the project were divided into sub tasks which are given as below:

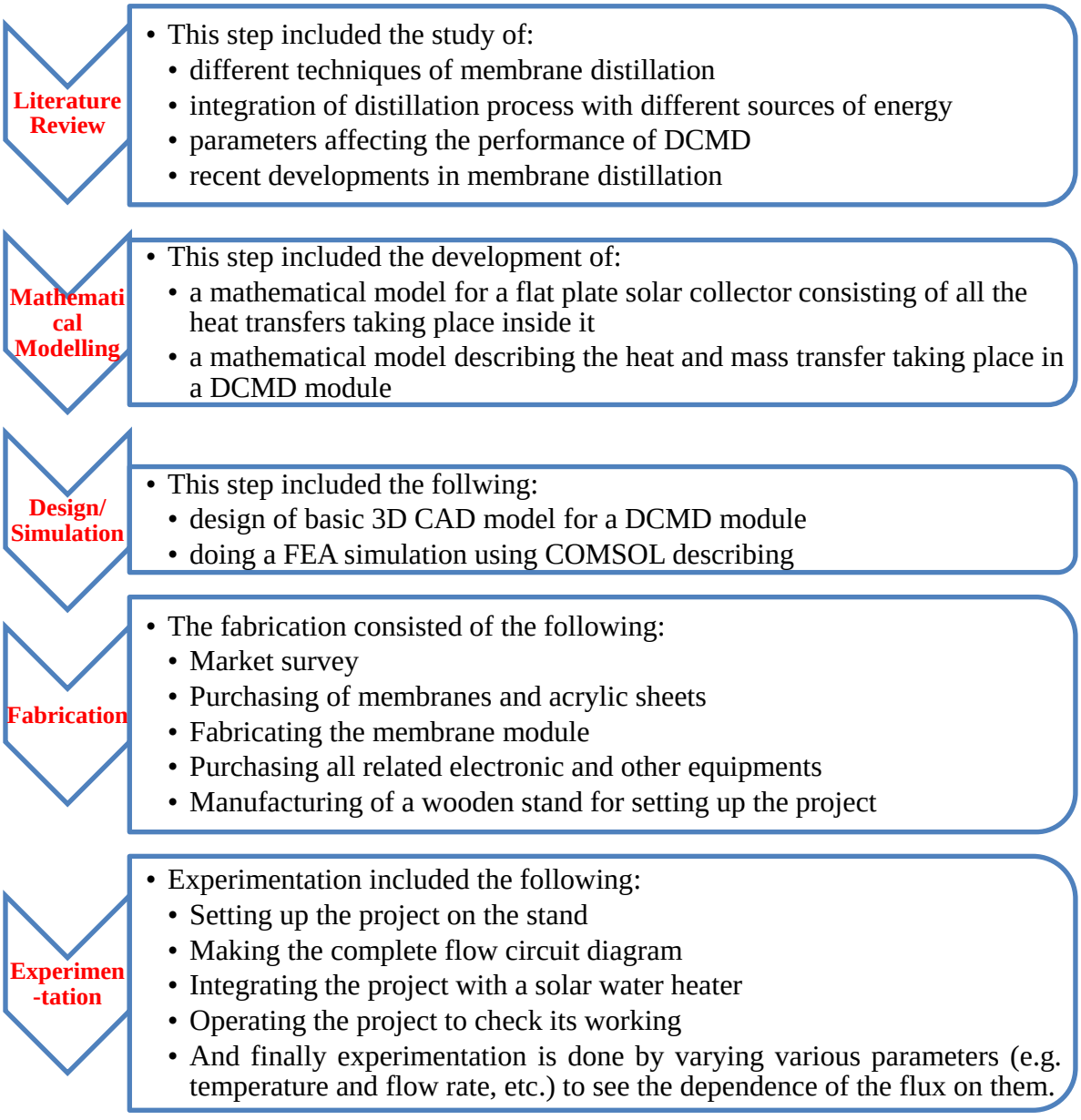

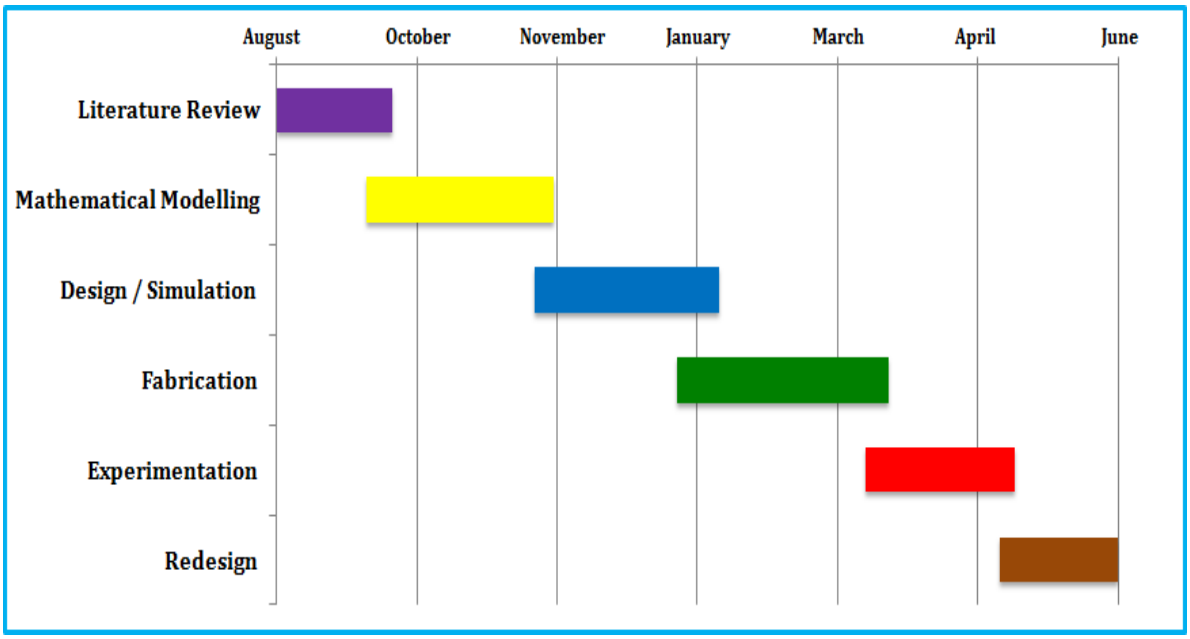

Figure 2: Gantt chart

CHAPTER 2: LITERATURE REVIEW

2.1 Membrane Distillation

Membrane distillation is a thermal driven process that accounts for the transport of vapors through hydrophobic membrane to get clean and pure water. It is regarded as one of the most atypical and nonpareil technologies that can succeed and replace the conventional methods that includes Multi stage flash (MSF), Reverse Osmosis etc. It is a topic of consideration since 1960 and a lot of versatile researches has been done on this premier method till today. However, despite the fact that it has not been able to get implemented in the industry, but still is now being considered as a prime topic for research due to its appealing features [7].

The role of operating conditions in membrane desalination process is extremely critical and thus was studied by Sulaiman et al. [8] in Direct Contact Membrane Desalination. They found that thermal efficiency and Transmembrane flux were found to be extremely delicate to feed temperature, feed flow rate and concentration of feed solution as increase in the first two properties enhanced thermal efficiency and Transmembrane flux and the latter one decreased the thermal efficiency and Transmembrane flux which was carried out on the modules named as MD020CP2N, MD020TP2N and MD080CO2N. They also studied the properties of hydrophobic membrane and found that increasing the thermal conductivity, thickness and decreasing the membrane porosity lessen the Tran's membrane flux and thermal efficiency. Similarly, different micro porous hydrophobic membranes of flat type of polyvinylidene fluoride (PVDF) and polytetrafluoroethylene (PTFE) were examined [9]. Drioli et al. [10] showed that low thermal conductivity, high liquid entry pressure, high thermal and chemical stability are the most favorable and suitable properties for hydrophobic membranes for the purpose of distillation.

Initially when membrane desalination was discovered in late 1960s, it was not commercialized particularly due to the fact that favorable and adequate properties of the membrane were an issue. So people started to look into the materials that can satisfy their

needs for the purpose of distillation. Hence, further research has been carried on to Nano materials by Daer et al. [11] and their studies have shown that they are superlative in salt rejection and contribute to high flux especially Zeolites, CNT's and Graphene. This can be extended to Reverse osmosis as well which can be carried out efficiently using GOF (Graphic Oxide Framework) rendered by molecular dynamics simulations [12].

Stand-alone membrane desalination process was constructed using mathematical model to investigate its potential by Alklaibi [13]. He developed the mathematical model which comprised of mass and heat transfer analysis. He proved that variation of different parameters and putting them in different equation yielded the outcome that polarization coefficient is minimum at relatively high Reynolds number. Drioli et al. [10] have explained that different nature of fouling occurs for different type of Membrane desalination methods.

A mathematical model was developed as well by Qtaishata et al. [14] using heat and mass analysis for locating the heat transfer coefficients values and interface temperature of the liquid/membrane. Model was evaluated on the basis of experimental evidences. It was solved using MATLAB and hence derived the result that permeate flux is highly dependent on average temperature. Similar results were deduced by Cai et al. [15] that feed temperature plays the most influential role on permeate flux. Also the dependency of mass transfer on heat transfer and relation between them was deliberated extensively. It was found using Dufour effect that it was insignificant at permeate and feed side under certain conditions whereas study of its effect is remarkable inside the membrane [16].

2.2 Vacuum Membrane Desalination

Various Vacuum Membrane Desalination (VMD) models have been developed and analyzed theoretically and experimentally. This word was first used by Bodell [17]. In one of the models, VMD model is suggested considering the bulk flow of temperature, velocity, mass fraction and pressure distribution as function of module length by Gil et al. [18]. The commercial membrane used was polypropylene (PP) hollow fiber type membrane module

from Mycrodyn-Nadir GmbH (MD020CP2N). They found that productivity increases with an increase in the inlet feed temperature (because of high vapor pressure difference) and velocity, the number of fibers and the total module length. However, it decreases with an increase in the mass fraction of the feed. VMD has been experimentally studied by M. Khayet et al. [19] and has determined the heat transfer coefficients in both the lumen and shell side of hydrophobic membrane.

2.3 Air Gap and Sweeping Gas Membrane Desalination

Similarly, other two types of membrane desalination are Air gap membrane desalination (AGMD) and Sweeping gas membrane desalination (SGMD) which have undergone a wide range of work and research on it. Effect of operating conditions in AGMD was examined by Khalifa et al. [20]. A novel method of AGMD using series and parallel connectors was analyzed by Khalifa el al. [21]. Similarly, Garcia et al. [22] modified the process with hollow fiber membrane made up of alumina. On the other side, SGMD has been studied with the assistance of theoretical and experimental studies as well as by modelling and optimization of different parameters [23, 24]. Sweeping gas MD using hollow fiber is comprehensively studied by Karinikola et al [25].

2.4 Permeate Gap and Conductive Gap Membrane Desalination

In addition to the above mentioned types of membrane desalination, there are other two types which have gained a lot of attention in the past few years i.e. Permeate Gap Membrane Desalination (PGMD) and Conductive Gap Membrane Desalination (CGMD) [10]. These two are considered to be the derived form of DCMD and AGMD and hence consists of the characteristics of both types of MD. One of the separating feature of these two types of MD is the distillate separation from the coolant. Also internal heat recovery is possible which makes them efficient from other forms of MD.

2.5 Comparison of different membrane distillation processes

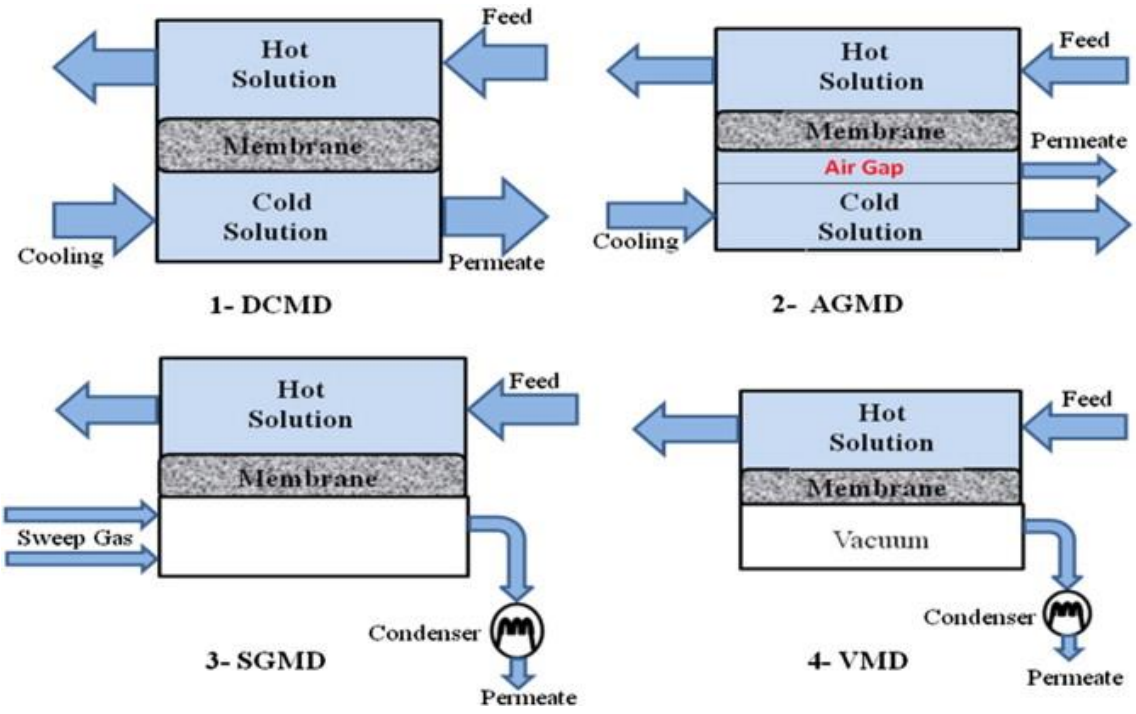

Figure 3: Comparison of different distillation processes

2.6 Other Advancements

Also there are other various advancements done in Membrane configuration and system for the purpose of improving the efficiency [26]. First of them is Vacuum enhanced DCMD in which setting the distillate pump right after the DCMD module causes an increase in the flux. The second innovation is Multi effect MD (MEMD). It is derived from AGMD having porous fibers arranged in the parallel form and dense wall fibers having an internal heat exchanging in the countercurrent direction. The other one is Vacuum- multi effect Membrane desalination (V-MEMD). It consists of both Multi effect distillation and Vacuum membrane desalination. Also Multi stage MD which is responsible for lowering the energy consumption. Osmotic MD requires a special mention in which vapor pressure difference is created with the help of water activity difference between the feed solutions.

Many renewable sources have been proposed to solve the energy problems [27]. Like the Solar energy which is the most abundant form and has been integrated in many of the MD related projects. Primarily the use of solar collector and PV cells have gained a lot of reputation in the recent years due to their enhanced ability to overcome cost and improve economical factor in Membrane desalination. Also Banat et al. has used solar still for producing potable water [28]. Geothermal energy which can offer the continuous thermal energy. However its extraction is little bit costly. Wind energy can serve the desalination plants in the form of electricity. Wave energy can serve as an ideal platform for membrane desalination plants. Similarly there are other forms of energy which can prove to play a vital role for solving the energy crisis related to MD and bring a revolution in future.

2.7 Solar driven Membrane systems

The concern of integrating membrane distillation with solar energy has been acclaimed a lot in the recent years. The major part of this activity comes from coupling the salinity gradient solar pond to membrane distillation [29]. Its effectiveness comes from energy consumption which mainly and primarily depends upon the average radiation of solar energy coming from sun as well as feed temperature. It also affects the economics aspects of using solar pond as a source of thermal energy for this process. Also the efficiency of the process is decreased as a result of thermodynamic losses. So this has been a subject of concern for others. For this purpose, Banat et al. did exergy analysis for the purpose of knowing the locations as well as causes of heat losses [30]. He revealed that the most obtrusive heat loss occurs primarily at the membrane module. Banat et al. also tried to integrate solar driven membrane distillation with artificial sea water [28]. The close loop system was adapted. Hot water was circulated in the unit of membrane distillation and this hot water was returned to the still. This showed quite superlative results if compared against nominal operative conditions.

Also two different categories of processes are devised by Qiblawey et al [31]. One of them was direct collection system and another one was indirect collection system. In direct

process, solar collector directly utilizes solar energy in order to generate distillate where in indirect process, there are two sub systems which are employed for producing distillate. One for desalination and the other one for solar energy collection. For limited water requirements, direct method is quite appropriate as it uses many versatile solar stills for producing clear and fresh water. The indirect method may use the electrical energy like photovoltaic cells for yielding sufficient electrical energy. It is further categorized into multi-stage flash distillation, atmospheric humidification and dehumidification etc. In addition to that, three different plants established in the span of two to three years were compared with each other with respect to membrane distillation configuration as well as energy supply [32]. Data was collected for all three plants and comparison was made with respect to distillate output, driving force temperature difference, Gain output ratio (GOR) and energy efficiency. From this, final outcome concerning the solar and waste heat driven plants for distillation was made for the purpose of optimum conditions.

Solar driven membrane distillation unit has also been coupled with air gap membrane distillation by Chang et al [33]. He basically took help from the proportional integral control scheme which is normally employed for the industries. The dynamic mathematical model helped to achieve the objective. This mathematical model was verified with experimental outcomes. The entire system as made automatic with this PI control scheme strategy under the influence of versatile irradiation conditions. This really assisted in determining the optimum conditions for running the system. Also vacuum membrane distillation has been integrated with solar energy by Wang [34] from underground water for potable and fresh water production. Basically the system was composed of four main critical components which included fiber hollow membrane module, solar energy collector, mechanical pumps and permeation condenser. The results showed very appreciable results and recommended this system a feasible one for the clean water production. Also simulation by coupling these two factors has been done by Mericqa et al [35] by considering solar gradient energy ponds with solar collectors. Basic outcome of the simulation was that temperature polarization phenomenon is the basic factor that decreases

and lessens the permeate flux because the process is not able to create sufficient turbulence due to the decrease of membrane interfaces temperatures and increase heat and energy loss.

Zhang then later compared the various sources of solar driven desalination and put the economic and physical benefits into the same platform [36]. He commented that indirect desalination technologies are becoming more and more reliable in future as there are technical improvements in water desalination technologies and simple technologies are preferable for rural areas. Also the total cost for producing potable water from solar collector is still relatively high as compared to the conventional and orthodox desalination methods. However, there is still a lot of space in cost reduction if used for large scale systems. Furthermore, low environmental disposal of residues and intermittence of solar energy with the continuous demand of water treatment are the major factors related to desalination of water. Similar type of analysis is done by Puoufaucon [37] in which he recommended continuous systems in place of discontinuous systems. Higher demands need a more sophisticated solar powered plant. However, there must be a balance between the solar electricity generation and electricity consumption. For this purpose, he endorsed that standalone systems are the most viable solution for producing potable water. Goswami [38] also revealed that solar hybrid desalination systems are much more economical than other systems but its yield depend upon weather, season and location. However there is a need of more research in this field especially related to operation of solar plant from waste heat and power cogeneration because both of them are very crucial areas if plants are operated on large scale.

The study of the evaporative cooling effect on the performance of solar driven membrane distillation unit was presented by Kabeel et al [39]. The study was basically carried out on pilot system. He observed the increase in the system productivity when incorporated with evaporative cooling effect. This phenomenon also caused an enhancement in Gain output ratio as well as system efficiency when compared with normal system at nominal flow rates. However the pressure drop was increased when flow rates were increased. Similarly the experimental investigation of solar ponds with direct contact membrane desalination

was done by Suarez [40]. Basically, he extracted the information regarding the water flux production as well as the energy requirements for the operation of basic components of system. DCMD incorporated with solar ponds is at least six times effective relative to AGMD. Also around 70% of the total energy generated from solar energy is used to drive the membrane system whereas 30% of the energy is lost during this process. Also around 50% of the useful heat is used to transport water across the membrane module and the rest is lost in the process of conduction in membrane. In addition to that, large membrane requires more capital cost to operate as compared to small membrane areas and better insulation could lead to better results as heat losses through the system will be reduced and water production will be much more effective.

The study of solar driven sea water distillation has also been done with the assistance of computer simulations via different softwares by Duong [41]. They extracted the results from various simulations that co-current and counter current flow of water in the system results in different profiles, thermal efficiency and thermal polarization factor as well. Direct contact membrane distillation is the best type to integrate with solar energy. In this regard, they have listed the best and the most viable setup for small scale production of potable water from distillation process. Also if the system is operated at relatively high temperature, then counter current flow is the most suitable one. Also if these configurations are regulated at high velocities, then water flux continues to increase until a steady value is reached. By examining different cases, they reached to a point that around an average of 19.7 kg of clean water per m^2 of membrane could be obtained in a day if operated under constant optimum conditions but that majorly depends on the radiation intensity of sun as well as availability of solar radiation during the day. Similar type of analysis has been done by Chang [42] in which he made the dynamic simulation model on Aspen Custom Modeler (ACM) for the optimum performance. He analyzed the different objective conditions on spiral type air membrane distillation and thus gave the most suitable conditions to achieve the paramount performance.

A very unique and exclusive sort of hybrid solar powered desalination system was designed by Chafidz et al. [43] for the purpose of providing fresh and potable water for remote and arid areas. The concept of zero energy has been used which does not address any sort of external energy but only and solely requires solar energy for its functioning. The idea of the system has been extracted from Memsys V-MEMD unit which has been integrated with solar photovoltaic system as well as solar collector. The heat pump was used to make the water flow from one part to another. The results were carried out on the basis of one day operation and outcomes were quite impressive if compared against other similar based systems. The average distillate flux was in the range of 1.5-2.5 $L/m^2.hr$. The solar efficiency of the system was around 33.6% which was comparatively less than other nominal systems. Similar form of analysis was carried out by Fath et al. [44] in which he performed closed direct contact air cycle. Basically he performed the experiments with the help of Humidifier and Dehumidifier. He drew the result from analysis that higher the solar intensity, higher will be the humidifier and dehumidifier effectiveness and thus larger will be the water production.

An effective but complex way of non-membrane process to produce potable water was done by Ayhan et al. [45] by Natural vacuum desalination. The advantage of this configuration was that in addition to sea water, sewerage water can be used. The cost of the water production is quite low but its limitations are that it requires removal of non-condensable gases which are formed during the water evaporation and handling of equipments is expensive. Guillen [46] studied the pilot scale MD solar distillation system by extensively analyzing three commercially prepared MD modules by coupling to an AGMD static solar collector field. The solution used was sodium chloride NaCl in a variety of ranges and the feed temperature up to 85^oC. The maximum amount of flux that was recorded was 7 $L/m^2.hr$ at the optimum operating conditions. A perspective of employing solar energy effectively was utilized by Shukla et al. [47] where he used the concept of latent heat energy storage in solar still for the purpose of producing clean and fresh water in the absence of sunlight. He did a lot of experiments on different forms of designs where

he viewed versatile economic and physical aspects. He observed an increase in the performance of solar still in this case. Also solar still technology was PCM based.

A short review of integrating solar energy with sustainable membrane desalination was done by Rahaoui [48] in which he has highlighted the trends of variation of different parameters on permeate flux. Temperature difference has an immense effect on heat transfer coefficients, mass lux, heat flux, evaporation efficiency and the most important one i.e. temperature polarization effect. All the factors increased with the enhancement of feed temperature but temperature polarization coefficient decreased with increase in feed temperature. Also coupling solar energy with any type of desalination is quite economical as compared to other normal systems and it is environmental friendly as well.

2.8 Analysis of Membrane desalination in different software's

As membrane desalination involves heat and mass transfer and dependency of mass transfer on heat transfer has been extensively studied under various conditions by Phattaranawik [16] that involve very complex PDE and ODE equations that have been solved using limited number of softwares only. Like DCMD equations have been first simplified by Qtaishat et al. [14] and thus solved using MATLAB. Also equations in the PDE form have been solved using COMSOL by Hasanizadeh et al [49] as it is a multiphysics software and thus can integrate heat and mass transfer at the same time in the same module as well.

On the other hand, for simulations, ANSYS Fluent and CFD have been extensively used. Like fluid flow effect on the permeate flux has been studied by Soukane et al. [50] in Fluent with turbulence model. Similarly, CFD analysis of DCMD has been done by H.Yu et al. [51] and have achieved very promising results that can be compared with experimental results. VMD analysis in CFD has been done by Hayer et al. [52] on the basis of fluid mechanics as well as heat and mass transfer.

2.9 Fouling and Wetting complications

Fouling of membranes is still one of the problems that torments the extensive stability of membranes and declines the flux. Its most common type is scale fouling. Its magnitude varies from one type of membrane desalination to another. Various methods were proposed to get rid to the maximum level by Tijing et al. [53] such as pretreatment, membrane flushing, gas bubbling etc.

Various versatile projects have tried to integrate the solar energy with Membrane desalination technology and have strived to provide new sagacity for diverse possible applications [54]. First commercial plant for MD was installed in Maldives in year 2014. Since then, a lot of plants have been established in various parts of the world to produce clean water. So Membrane desalination is an effective technique that if employed, can produce the clean and pure water safe for drinking and thus can solve the drinking issues at present and in future as well.

CHAPTER 3: METHODOLOGY

3.1 SCHEMATIC DIAGRAM

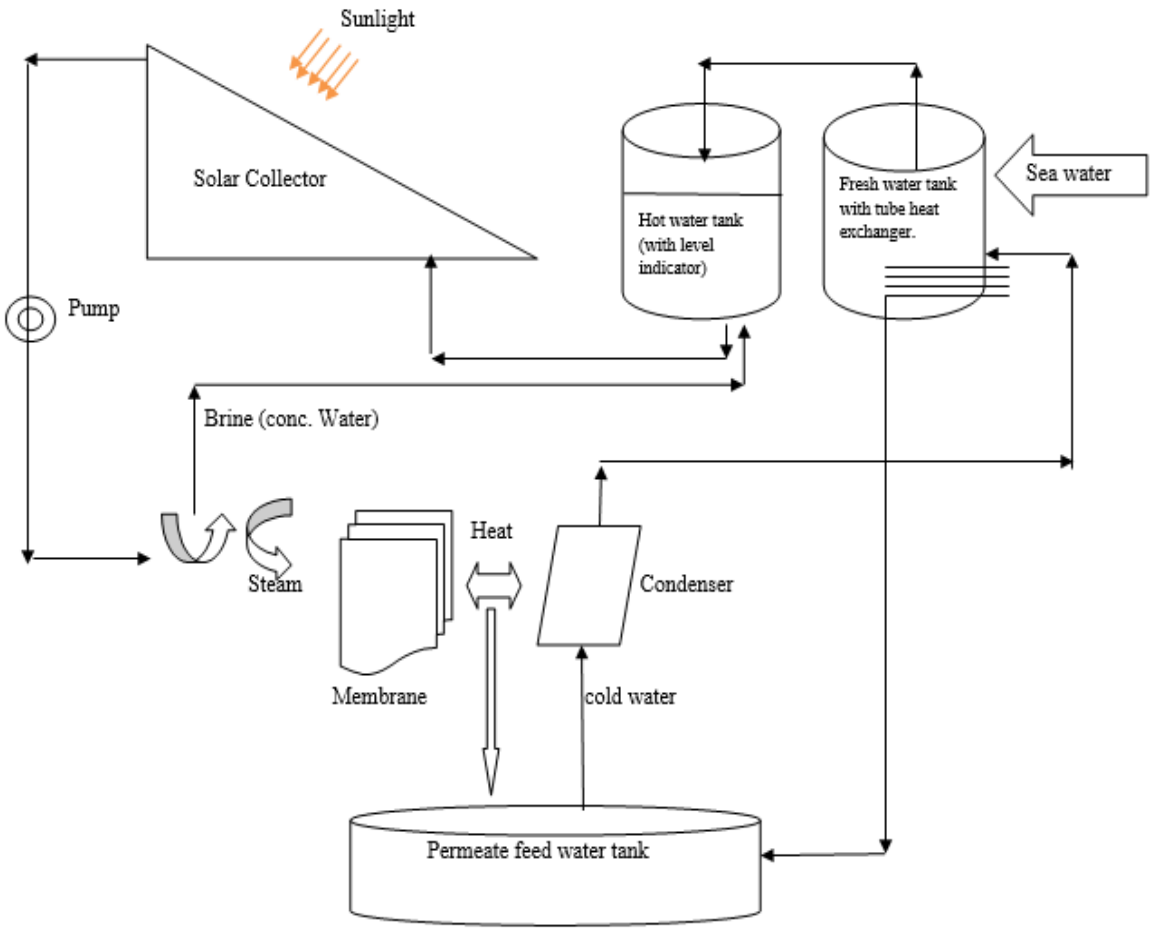

Figure 4: Schematic diagram

3.1.1 Working cycle

- The main working component in the cycle of membrane desalination is porous hydrophobic membrane.
- Fresh water (to be purified) is initially stored in fresh feed water tank having tubes hence it also acts as shell and tube heat exchanger.

- Hot feed water tank is connected with F.W.T to maintain water level in H.F.W.T.
- Water is heated to 50-60 Degree Celsius through solar panel and pumped to the feed side of membrane which allows only vapors to pass through it.
- Concentrated water (brine) is pumped back to H.F.W.T which also decreases pressure in it (helps in formation of vapors).
- Condenser on the permeate side of membrane condenses the pure vapors using cold water from permeate water tank (purified) and exchanges heat. This heated water (because of condensation) is also used to pre heat the fresh water in F.W.T (Heat Recovery).
- The process is a closed loop as well as standalone process. All the above steps are repeated as described above.

3.2 CAD MODEL

To use membranes practically, large membrane area is needed. The smallest section into which a membrane area is packed is called a module. A module typically consists of membrane, feed inlet, permeate outlet and a supporting structure which provides the necessary support to the whole unit. There are different configurations present in the literature for a membrane module. Some of these configurations include; hollow fiber module, spiral wound module, plat and frame module and tubular module.

We will be using plat and frame (cross-flow) module configuration. A 3D model of the proposed model is shown in **Figure 3**. In this configuration, two rectangular plates are present on both sides to provide necessary support to the module during the operation. Spacers are also used on either sides and the membrane is enclosed in between the two spacers. In membrane distillation, thermal polarization is one of the important factors which limit the performance of the distillation process by reducing the thermal driving force. Spacer helps to decrease the temperature polarization by increasing the heat transfer

which results in higher permeate flux. The whole geometry will be assembled together tightly with the help of nuts and bolts to prevent any leakage and disturbing of membrane sheet during the operation.

The parts labeled in the figure are as:

1) Supporting plate
2) Spacer
3) Membrane Sheet

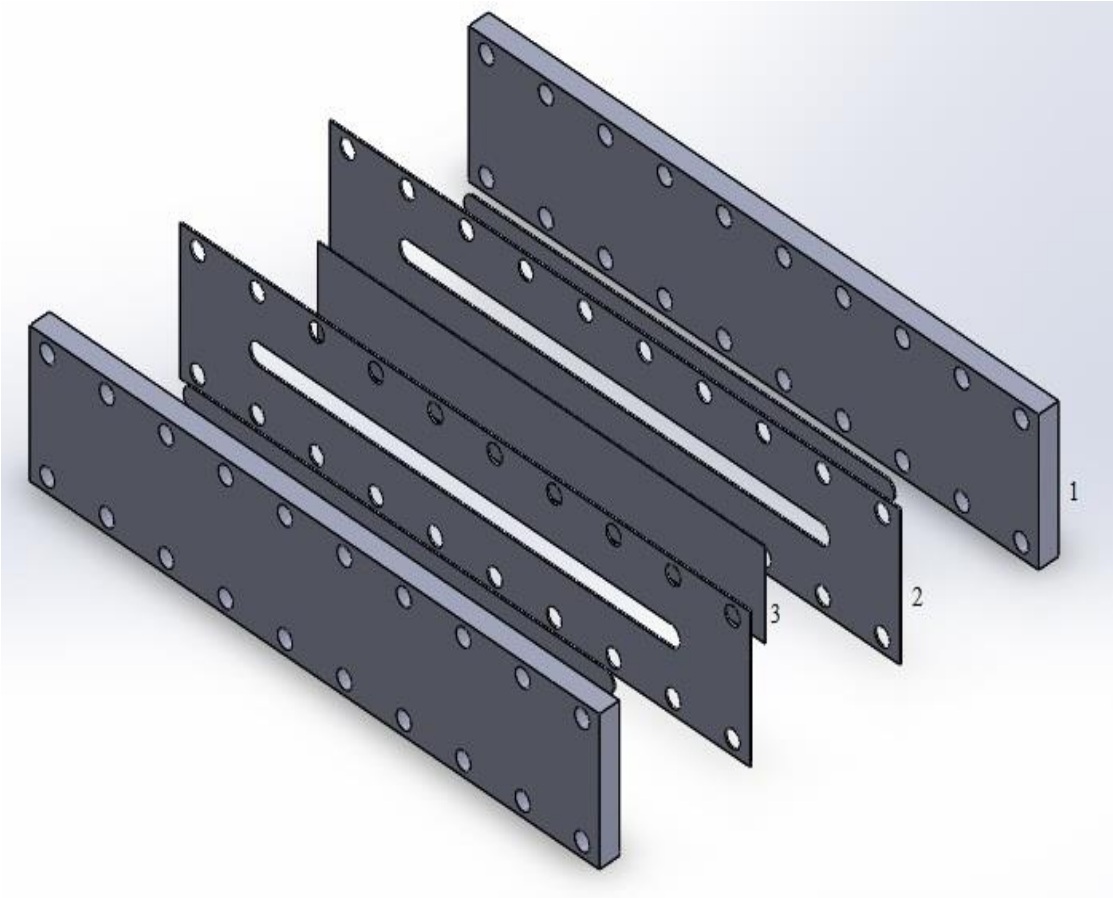

Figure 5: CAD Model

3.3 MATHEMATICAL MODELLING

3.3.1 Mathematical modeling of DCMD

As Membrane desalination is a process that occurs due to the pressure difference created due to the temperature difference across feed and permeate side so analysis can be split into three different regions. **(1)** Feed side Heat transfer (includes heat transfer through convection $Q_{f,conv.}$ as well as it incorporates mass transfer which governs the second type of heat transfer$Q_{f,M.T.}$); **(2)** Heat transfer in membrane (includes heat transfer through conduction $Q_{m,cond.}$ and transfer of heat due to the passage of water vapors through pores of membrane $Q_{m,M.T.}$); **(3)** Transfer of heat in permeate side (includes convectional heat transfer $Q_{p,conv.}$ as well as transfer of mass governs the second type of heat transfer across permeate boundary$Q_{p,M.T.}$) [14].

They can be expressed in the form of mathematical equations as well as stated below;

- feed side:

$$Q_f = Q_{f,conv.} + Q_{f,M.T.} = h_f\left(T_{bf} - T_{mf}\right) + J_w H_{L,f}\left\{\frac{T_{bf} + T_{mf}}{2}\right\} \qquad \textbf{\textit{Eq. 1}}$$

- membrane:

$$Q_m = Q_{m,cond.} + Q_{m,M.T.} = h_m\left(T_{mf} - T_{mp}\right) + J_w H_v \qquad \textbf{\textit{Eq. 2}}$$

- permeate side:

$$Q_p = Q_{p,conv.} + Q_{p,M.T.} = h_p\left(T_{mp} - T_{bp}\right) + J_w H_{L,p}\left\{\frac{T_{mp} + T_{bp}}{2}\right\} \qquad \textbf{\textit{Eq. 3}}$$

In literature, it has been determined that the type of heat transfer that dominates is the convection heat transfer on both sides of membrane [55]. Hence we can eradicate the terms of conduction for both sides.

Moreover, the enthalpy of vapor H_v is regarded as approximately equal to latent heat of vaporization (ΔH_v). Based on this approximation, the Eq. [(1-3)] can be rewritten as follows:

$$Q_f = h_f(T_{bf} - T_{mf}) \qquad \textbf{Eq. 4}$$

$$Q_p = h_p(T_{mp} - T_{bp}) \qquad \textbf{Eq. 5}$$

$$Q_m = h_m(T_{mf} - T_{mp}) + J_w \Delta H_v \qquad \textbf{Eq. 6}$$

In correspondence to the above equations, the average bulk feed temperature T_{bf} is the average of bulk inlet and bulk outlet flow temperatures:

$$T_{bf} = \frac{T_{bf,in} + T_{bf,out}}{2} \qquad \textbf{Eq. 7}$$

Similarly, for average bulk permeate temperature T_{bp}:

$$T_{bp} = \frac{T_{bp,in} + T_{bp,out}}{2} \qquad \textbf{Eq. 8}$$

Coefficient of heat transfer plays a very pivot role in heat transfer across the membrane and controls the flux through the membrane. Its evaluation is done with the help of thermal conductivity of the material k_m from which membrane is made as well as the air which is trapped inside the membrane k_g. Its equation is given as follows:

$$h_m = \frac{k_g \varepsilon + k_m(1 - \varepsilon)}{\delta} \qquad \textbf{Eq. 9}$$

For finding the shell and lumen side heat transfer coefficients($h_f \; and \; h_p$), we would take help of various dimensionless numbers [56] like Nusselt Number, Prandtl Number etc.

Reynolds Number (i=feed, permeate):

$$Re_i = \frac{\rho_i v_i d_i}{\mu_i} \qquad \textbf{Eq. 10}$$

Prandtl Number (i=feed, permeate):

$$Pr_i = \frac{\mu_i Cp_i}{k_i} \qquad \textbf{Eq. 11}$$

Nusselt Number –laminar flow (i=feed, permeate):

$$Nu_i = 1.86\left(\frac{Re_i Pr_i d_i}{l_i}\right)^{0.33} \qquad \textbf{Eq. 12}$$

Nusselt Number –turbulent flow (i=feed, permeate):

$$Nu_i = 0.023(Re_i)^{0.8}(Pr_i)^{0.33}\left(\frac{\mu i}{\mu si}\right)^{0.14} \qquad \textbf{Eq. 13}$$

Heat transfer coefficients (i=feed, permeate):

$$h_i = \frac{Nu_i k_i}{d_i} \qquad \textbf{Eq. 14}$$

Heat of vaporization of water ΔH_v is an experimental factor but certain relations exists which operate only in the certain temperature range. The following relation operates in the 273K-373K temperature range. Its evaluation is done on the average temperature between feed and permeate side as follows [55, 57]:

$$\Delta H_v = 1.7535T + 2024.3 \qquad \textbf{Eq. 15}$$

Where mean temperature between bulk feed and permeate side is represented by T as:

$$T = \frac{T_{bf} + T_{bp}}{2} \qquad \textbf{Eq. 16}$$

At steady state:

$$Q_f = Q_m = Q_p = Q \qquad \textbf{Eq. 17}$$

Combining equations [Eq. (4-6)] in Eq. 17 the heat becomes:

$$Q = h_f(T_{bf} - T_{mf}) = h_p(T_{mp} - T_{bp}) = h_m(T_{mf} - T_{mp}) + J_w \Delta H_v \qquad \textbf{Eq. 18}$$

Solving for Q, we get the following equation:

$$Q = \left(\frac{1}{h_f} + \frac{1}{h_m + \frac{J_w \Delta H_v}{T_{mf} - T_{mp}}} + \frac{1}{h_p} \right)^{-1} (T_{bf} - T_{bp}) \qquad \textbf{Eq. 19}$$

Also one factor that is interconnected to heat flux is overall heat transfer coefficient U which is a very critical factor as indicated below:

$$U = \left(\frac{1}{h_f} + \frac{1}{h_m + \frac{J_w \Delta H_v}{T_{mf} - T_{mp}}} + \frac{1}{h_p} \right)^{-1} \qquad \textbf{Eq. 20}$$

The mass flux J_w is dependent on two very important factors in this process i.e. first is mass transfer coefficient (Viscous model, Knudsen model, ordinary-diffusion model or their pair) and second is pressure difference across membrane. It is calculated by [55,58]:

$$J_w = B_m(P_{mf} - P_{mp}) \qquad \textbf{Eq. 21}$$

Evaluation of partial pressure is governed by Antoine equation which converts the temperature of any side into partial pressure of that side as shown below:

$$P^v = \exp\left(23.328 - \frac{3841}{T - 45}\right) \qquad \textbf{Eq. 22}$$

There exist many different types of governing mechanisms to represent mass transfer through a porous media: Viscous model, Knudsen model, ordinary-diffusion model and may be a combination as well. Knudsen number K_n is responsible for calculating which type of mechanism governs the mass transfer. It is dependent on two things i.e. mean free path of molecules λ and membrane pore size diameter d [14]:

$$K_n = \frac{\lambda}{d} \qquad \textbf{Eq. 23}$$

In our model, we are using a combination of Knudsen model and ordinary diffusion model. So membrane permeability B_m for combined Knudsen-ordinary diffusion is given by the following equation:

$$B_m^C = \left[\frac{3}{2}\frac{\tau\delta}{\varepsilon r}\left(\frac{\pi RT}{8M}\right)^{\frac{1}{2}} + \frac{\tau\delta}{\varepsilon}\frac{P_a}{PD}\frac{RT}{M}\right]^{-1} \qquad \textbf{Eq. 24}$$

Where P_a represents the air which is trapped inside the membrane pores and D is the water diffusion coefficient. Water-air PD value is given as [16] which will then be substituted in the above equation:

$$PD = (1.895 \times 10^{-5})T^{2.072} \qquad \textbf{Eq. 25}$$

Membrane tortuosity τ is primarily dependent on porosity of membrane and it can be calculated by using the following correlation [55]:

$$\tau = \frac{(2-\varepsilon)^2}{\varepsilon} \qquad \textbf{Eq. 26}$$

As coefficient of heat transfer is dependent on conductivity of the material from which membrane is composed k_m as well as the air which is trapped inside the membrane k_g. Similarly, membrane's ability to conduct heat k_m is also dependent on these factors. Hence

$$k_m = \varepsilon k_g + (1-\varepsilon)k_p \qquad \textbf{Eq. 27}$$

So by putting all the values of parameters in Knudsen- ordinary diffusion model and then replacing its values in mass flux equation along with the result of Antoine equation for feed and permeate side, we could obtain the mass flux J_w at desired temperatures. Also, evaluation of other parameters is dependent primarily on membrane interfaces temperatures and the mass flux.

One of the most critical and pivot element that influences the effectiveness and efficiency of this system is the Temperature Polarization Coefficient (TPC) which heavily affects and decreases the permeate flux passing across hydrophobic membrane [14]. Heat losses that occur during the process are responsible for the bulk temperatures to be not equal to the membrane interfaces temperatures. This phenomenon is actually known as TPC which is a factor responsible for the effectiveness of process. It is dependent on membrane interface temperatures and bulk temperatures on both sides. It is stated as follows:

$$TPC = \frac{T_{mf} - T_{mp}}{T_{bf} - T_{bp}} \qquad \textbf{Eq. 28}$$

The evaporation efficiency EE can be delineated as portion of heat that is migrated due to water vapors passing across the membrane out of total heat transferred [59]:

$$EE = \frac{Q_{m,M.T}}{Q_{m,M.T} + Q_{m,cond.}} = \frac{J_w H_v}{J_w H_v + h_m(T_{mf} - T_{mp})} \qquad \textbf{Eq. 29}$$

For finding the rate of total heat transferred through hydrophobic membrane, we will use the following equation:

$$q_t = U(T_{bf} - T_{bp}) \qquad \textbf{Eq. 30}$$

Where U is the overall heat transferred coefficient which is determined with the help of Eq. (20).

To solve these equations in MATLAB it requires an iterative scheme of many equations and combination of many variables. To make it easy in solving in this software, following pivot equations are derived from the above equations. The extensive iterative process is used to evaluate these temperatures of both sides of the hydrophobic membrane.

On feed side:

$$T_1 = \frac{h_m(T_p + (h_f/h_p)T_f) + h_f T_f - JH_v}{h_m + h_f(1 + h_m/h_p)} \qquad \textbf{\textit{Eq. 31}}$$

On permeate side:

$$T_2 = \frac{h_m(T_f + (h_p/h_f)T_p) + h_p T_p + JH_v}{h_m + h_p(1 + h_m/h_f)} \qquad \textbf{\textit{Eq. 32}}$$

3.3.1.1 Overview of modeling of membrane distillation in MATLAB

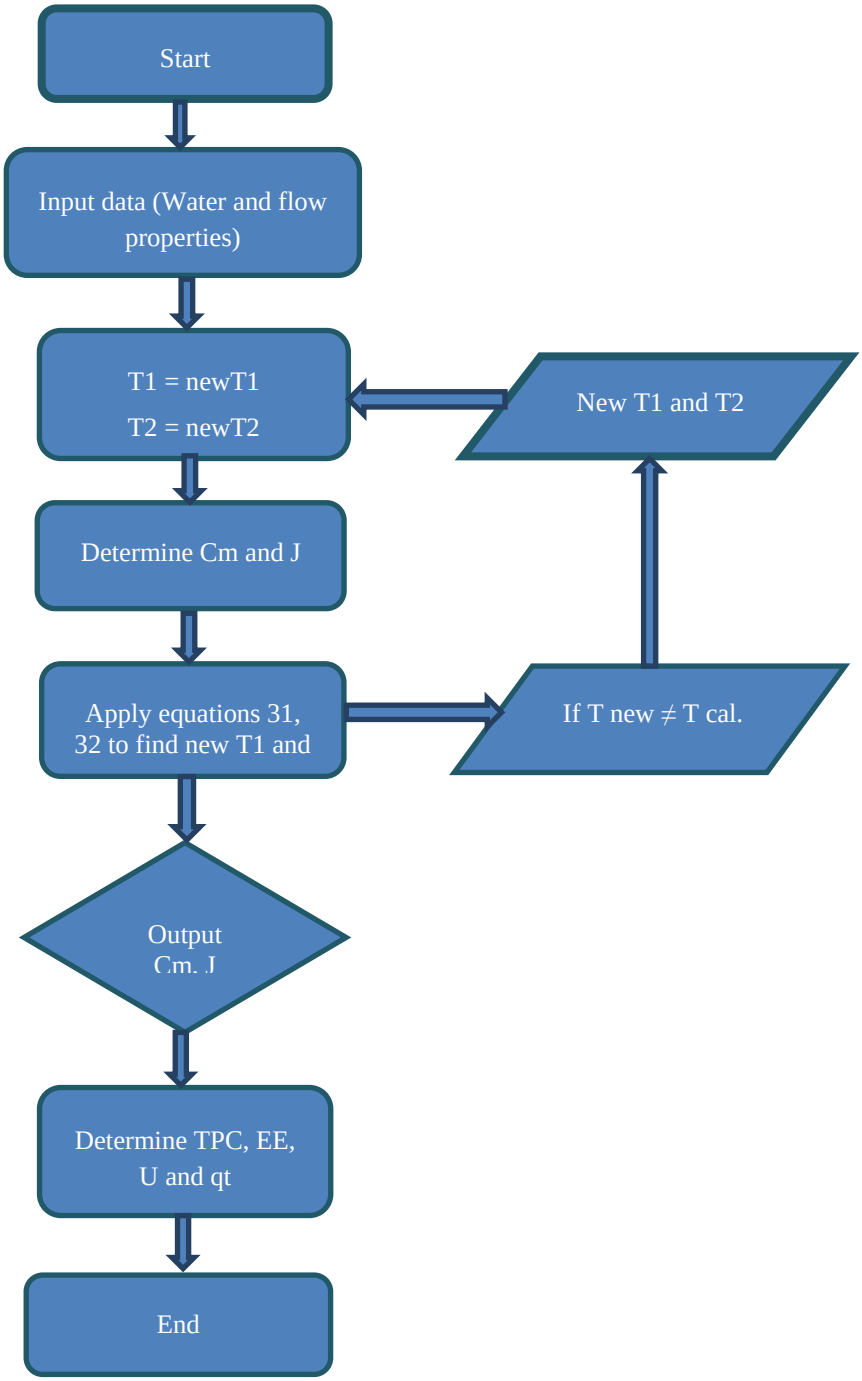

Figure 6: Membrane Distillation Flow chart in MATLAB

An iterative scheme has been used to find the flux over a vast range of temperatures.

- All the water properties and flow characteristics are inputted in the beginning.
- As an initial guess, values of T_{mf}, T_{mp} are inputted after this.
- These Temperatures and water parameters contribute to determine Knudsen – Ordinary diffusion coefficient as well as Mass flux.
- Mass flux value will lead us to new membrane interfaces temperature.
- Then it is checked whether the new temperatures calculated are equal or close to (within tolerance of 1e-04) to the previous membrane temperatures.
- If the condition is not satisfied, then steps (2-5) are repeated again in such a manner that the new temperatures are set equal to the old temperatures.
- The above steps will continue until and unless the difference between the old and new temperatures gets less than or equals to 1e-04 (tolerance).
- If the condition is satisfied then these temperatures are the true or close to true membrane interfaces temperatures. These temperatures are proceeded further to calculate the actual amount of flux pass across the membrane.
- These temperatures are then further engaged to find other valuable parameters like Evaporator Efficiency (EE), Thermal Polarization coefficient (TPC) etc.

3.3.2 Mathematical modeling of solar collector

The energy requirements for the DCMD module are met by integrating the system with solar collector. All solar collectors have same working principle. The black surface (absorber plate) absorbs the radiations coming from Sun; performs the heating operation and transfer this heat to any fluid that is moving through the pipes. The pivot elements of a solar collector (flat plate) include: glass covering, absorber, piping and housing of the system. The absorber is protected with a thin sheet that consumes the solar radiations. The glass covering protects the collector form external conditions and also prevents heat loss from it. The glass cover should have high permeability for the solar radiations, so that maximum sun rays are transmitted through it on their way to the absorber plate. A system

of pipes containing the fluid collects heat from the absorber. The arrangement of pipes may be parallel or they may be arranged in a coiled system. The housing of the system protects and prevents any sort of losses during its operation of heating the fluid. It comprises of typical insulation around the solar collector which ensures low heat losses.

Following assumptions were made to simplify the analysis of a solar collector [60];

- Collector tubes have unit mass flow rate.
- Heat transfer throughout the system takes place in one dimension.

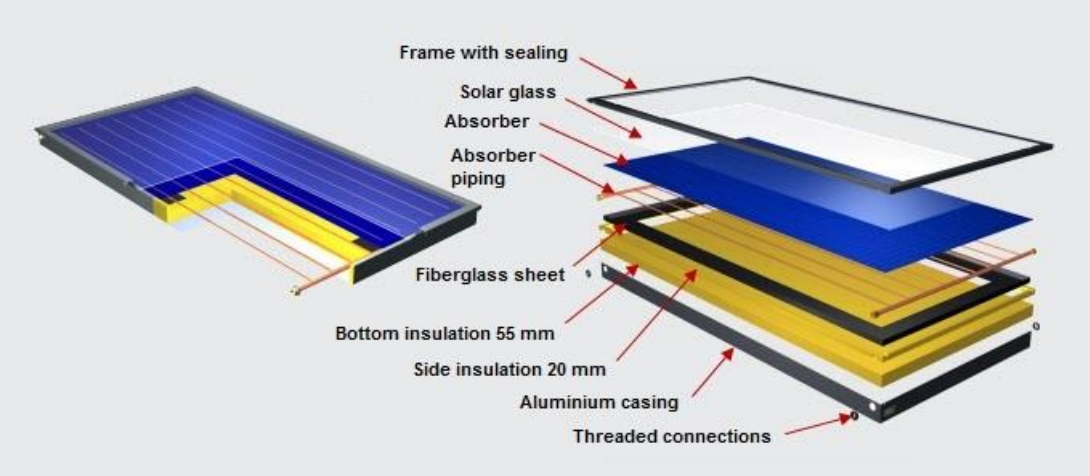

Figure 7: Break down of Solar collector

- The heat transfer as well as heat losses from the collector edges are neglected.
- Temperature does not affect characteristics of glass and insulation.

General energy balance for one dimensional heat transfer can be written as:

$$\frac{dU}{dx} = \dot{Q}_{in} - \dot{Q}_{out} + \dot{Q}_{v} \qquad \textbf{Eq. 33}$$

The heat transfer across the solar collector's glass cover can be written as [61]:

$$c_g V_g \rho_g \frac{dT_g}{dt} = \left[h_{g,am}(T_{am} - T_g) - h_{r1}(T_g - T_{ab}) - h_{c1}(T_g - T_a) + G\alpha\right] p\Delta z \qquad \textbf{Eq. 34}$$

The air gap between the absorber plate and glass cover also yields some heat transfer as:

$$c_a(T_a)V_a\rho_a(T_a)\frac{dT_a}{dt} = \left[h_{c1}\left(T_g - T_a\right) - h_{g,ab}\left(T_a - T_g\right)\right]p\Delta z \qquad \textbf{Eq. 35}$$

Now considering the plate (absorber), the heat absorbed by the plate is a result of radiation heat transfer between the absorber and glass cover, process of conduction between insulation and absorber and heat transfer by process of convection. Thus:

$$\begin{aligned} c_{ab}(T_{ab})V_{ab}\rho_{ab}(T_{ab})\frac{dT_{ab}}{dt} \\ = \Big[G(\alpha\tau) - h_{r1}\left(T_{ab} - T_g\right) - h_{c1}(T_{ab} - T_a) \\ - \frac{k_i}{\delta_i}(T_{ab} - T_i)\Big]p\Delta z - \pi d_{in}h_f\Delta z\left(T_{ab} - T_f\right) \end{aligned} \qquad \textbf{Eq. 36}$$

The heat transfer in the insulation zone consists of conduction heat transfer with the absorber plate and radiation heat transfer with the surrounding environment:

$$c_i\rho_i V_i\frac{dT_i}{dt} = \frac{k_i}{\delta_i}(T_{ab} - T_i) + h_{i,am}(T_{am} - T_i) \qquad \textbf{Eq. 37}$$

The energy balance for the working fluid in the solar collector is given by:

$$c_f\left(T_f\right)\rho_f\left(T_f\right)A\frac{\partial T_f}{\partial t} = \pi d_{in}h_f\left(T_{ab} - T_f\right) - \dot{m}_f c_f\left(T_f\right)\frac{\partial T_f}{\partial z} \qquad \textbf{Eq. 38}$$

Applying the First law of thermodynamics across the control volume of the storage tank:

$$\frac{dE_{cv}}{dt} = \dot{m}_{in}\left(h + \frac{V^2}{2} + gz\right) - \dot{m}_{out}\left(h + \frac{V^2}{2} + gz\right) + \dot{Q} - \dot{W} \qquad \textbf{Eq. 39}$$

Any sort of changes in kinetic and potential energy are neglected. Also there is no work done in the system in storage tank case, so the above energy balance can be stated as:

$$\frac{d(mu)_{cv}}{dt} = \dot{Q}_{loss} + \dot{m}_{in}h_{in} - \dot{m}_{out}h_{out} \qquad \textbf{Eq. 40}$$

Finite difference method is used to solve the differential equations. The geometry and time derivatives are replaced by backward and forward difference formula, respectively:

$$\frac{dT_m}{dt} = \frac{T_{m,j}^{t+\Delta t} - T_{m,j}^{t}}{\Delta t} \qquad \textbf{Eq. 41}$$

$$\frac{dT_f}{dz} = \frac{T_{f,j}^{t+\Delta t} - T_{f,j}^{t}}{\Delta z} \qquad \textbf{Eq. 42}$$

The final form of the equations using finite difference method becomes [61]:

$$T_{g,j}^{t+\Delta t} = \frac{1}{F_j \Delta t} T_{g,j}^{t} + \frac{B_j}{F_j} T_{am}^{t+\Delta t} + \frac{C_j}{F_j} T_{ab,j}^{t+\Delta t} + \frac{D_j}{F_j} T_{a,j}^{t+\Delta t} + \frac{E}{F_j} G^{t+\Delta t} \qquad \textbf{Eq. 43}$$

$$T_{a,j}^{t+\Delta t} = \frac{1}{H_j \Delta t} T_{a,j}^{t} + \frac{G_j}{H_j}\left(T_{g,j}^{t+\Delta t} + T_{ab,j}^{t+\Delta t}\right) \qquad \textbf{Eq. 44}$$

$$T_{ab,j}^{t+\Delta t} = \frac{1}{Q_j \Delta t} T_{ab,j}^{t} + \frac{K_j}{Q_j} G^{t+\Delta t} + \frac{L_j}{Q_j} T_{g,j}^{t+\Delta t} + \frac{M_j}{Q_j} T_{a,j}^{t+\Delta t} + \frac{O_j}{Q_j} T_{f,j}^{t+\Delta t} + \frac{P_j}{Q_j} T_{i,j}^{t+\Delta t} \qquad \textbf{Eq. 45}$$

$$T_{f,j}^{t+\Delta t} = \frac{1}{U_j \Delta t} T_{f,j}^{t} + \frac{R_j}{U_j} T_{ab}^{t+\Delta t} + \frac{S_j}{U_j \Delta z} T_{f,j-1}^{t+\Delta t} \qquad \textbf{Eq. 46}$$

$$T_{i,j}^{t+\Delta t} = \frac{1}{X_j \Delta t} T_{i,j}^{t} + \frac{V_j}{X_j} T_{ab}^{t+\Delta t} + \frac{W_j}{X_j} T_{am}^{t+\Delta t} \qquad \textbf{Eq. 47}$$

Where $j = 1,2,3, \dots, N$

$$T_{tank}^{t+\Delta t} = \frac{\dot{m}_{tot} c_p(t_f)}{m_{tank} c_v(t_f)} \Delta\tau \left(T_{f,n}^{t} - T_{tank}^{t}\right) - h_{tank,amb} \frac{A_{tank}}{m_{tank} c_v(t_f)} \Delta\tau (T_{tank}^{t} + T_{am}^{t}) + T_{tank}^{t} \qquad \textbf{Eq. 48}$$

The coefficients used in the above equations are:

$$B_j = \frac{h_{g,am.j}}{c_g \rho_g V_g} \qquad \textbf{Eq. 49} \qquad \boldsymbol{C_j = \frac{h_{r1.j}}{c_g \rho_g V_g}} \qquad \textbf{Eq. 50}$$

$$D_j = \frac{h_{c1.j}}{c_g \rho_g V_g} \qquad \textbf{Eq. 51} \qquad \boldsymbol{E_j = \frac{\alpha}{c_g \rho_g V_g}} \qquad \textbf{Eq. 52}$$

$$F_j = \frac{1}{\Delta t} + B_j + C_j + D_j \qquad \textbf{Eq. 53}$$

$$\boldsymbol{H_j = \frac{1}{\Delta t} + 2G_j} \qquad \textbf{Eq. 54}$$

$$G_j = \frac{h_{c1.j}p}{c_a(T_a)_j\rho_a(T_a)_j(p\delta_{ab} + \pi r_{out}^2)} \qquad \textbf{Eq. 55}$$

$$J_j = c_{ab}(T_{ab})_j\rho_{ab}(T_{ab})_j[p\delta_{ab} + \pi(r_{out}^2 - r_{in}^2)] \qquad \textbf{Eq. 56}$$

$$K_j = \frac{p(\tau\alpha)}{J_j} \qquad \textbf{Eq. 57}$$

$$\boldsymbol{L_j = \frac{h_{r1j}p}{J_j}} \qquad \textbf{Eq. 58}$$

$$M_j = \frac{h_{c1.j}p}{J_j} \qquad \textbf{Eq. 59}$$

$$\boldsymbol{O_j = \frac{\pi d_{in}h_{f,j}}{J_j}} \qquad \textbf{Eq. 60}$$

$$P_j = \frac{pk_i}{J_j\delta_j} \qquad \textbf{Eq. 61}$$

$$Q_j = \frac{1}{\Delta t} + L_j + M_j + O_j + P_j \qquad \textbf{Eq. 62}$$

$$R_j = \frac{\pi d_{in}h_{f,j}}{c_f(T_f)_j\rho_f(T_f)_jA} \qquad \textbf{Eq. 63}$$

$$S_j = \frac{\dot{m}_f}{\rho_f(T_f)_jA} \qquad \textbf{Eq. 64}$$

$$U_j = \frac{1}{\Delta t} + R_j + \frac{S_j}{\Delta z} \qquad \textbf{Eq. 65}$$

$$V_j = \frac{2k_i}{c_i\rho_i\delta_i^2} \qquad \textbf{Eq. 66}$$

$$W_j = \frac{2h_{i,am,j}}{c_i\rho_i\delta_i} \qquad \textbf{Eq. 67}$$

$$X_j = \frac{1}{\Delta t} + V + W_j \qquad \textbf{Eq. 68}$$

These equations are solved by an iterative process using MATLAB®. This forms the basis of MATLAB® code as well. The stopping criterion for this iterative process is:

$$\left|\frac{T_{j,(k+1)}^{t+\Delta t} - T_{j,(k)}^{t+\Delta t}}{T_{j,(k+1)}^{t+\Delta t}}\right| \leq \vartheta \qquad \textbf{Eq. 69}$$

Also the entire process has to satisfy the Courant-Lewy-Friedriches condition as well:

$$|\psi| < 1 \ \ where\ \psi = \frac{\omega_f\Delta t}{\Delta z} \qquad \textbf{Eq. 70}$$

3.3.2.1 Overview of modeling of solar collector in MATLAB

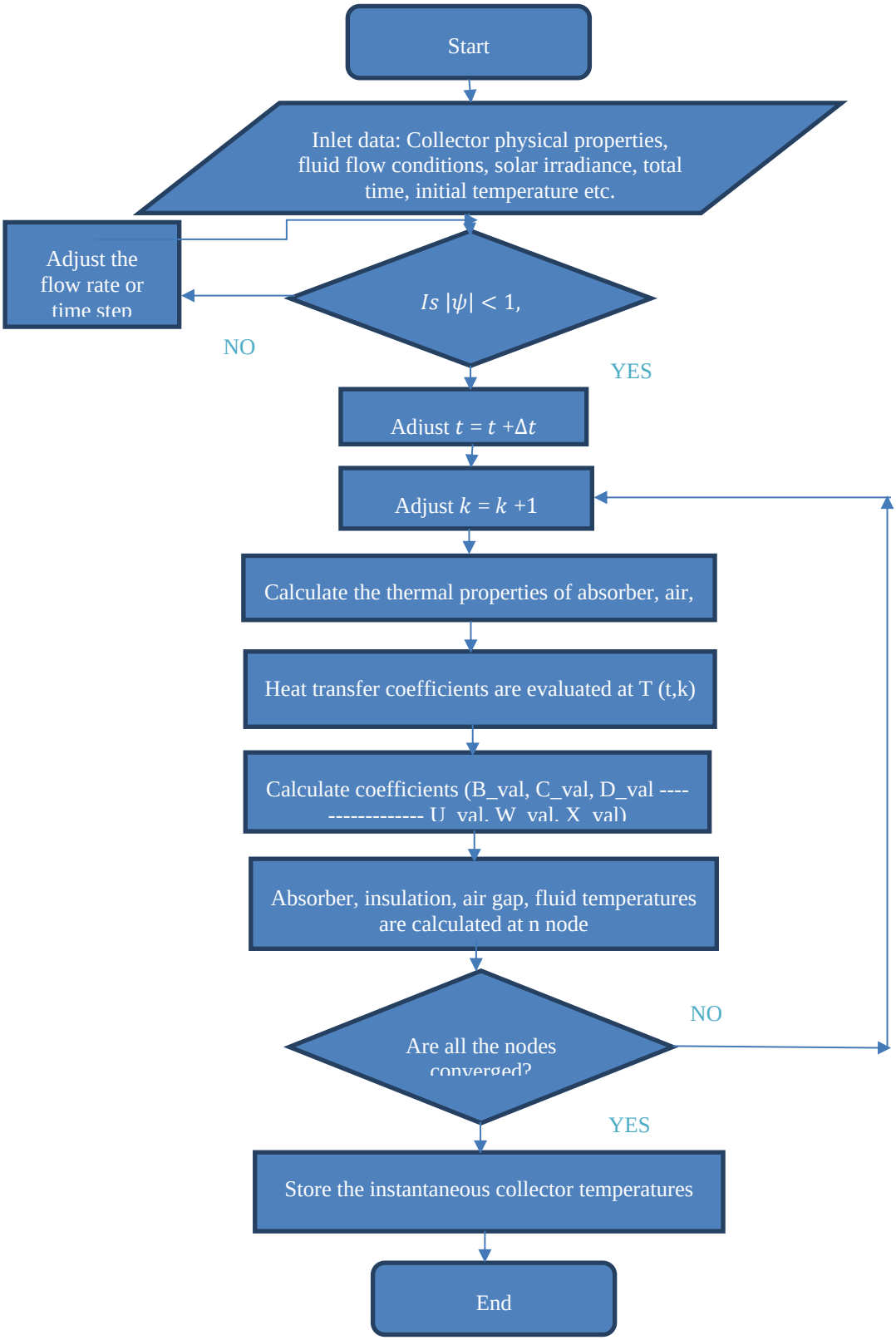

Figure 8: Solar collector Flow chart in MATLAB

3.3.3 FINITE ELEMENT MODELLING IN COMSOL

All the derived equations as well as boundary and initial conditions are solved with the assistance of Finite Element Method (FEM) using **COMSOL Multiphysics 5.0 package**. COMSOL utilizes the Finite Element Method to solve the model equations on the basis of numerical methods. The incisiveness of this method in COMSOL software depends relatively upon how effectively one has put the initial and boundary conditions factual.

As we all know that in Finite element modelling, the whole domain is divided into finite control element. Same case is applied here in which mesh is generated of standard level to segregate the system into many control elements on the basis of to what extent we want accuracy in results and reduce numerical lapse in results. After this, complex Partial differential equation, which are otherwise pretty difficult to solve manually are being converted into Algebraic equations within COMSOL and thus have generated the numerous results which are accumulated in the next section

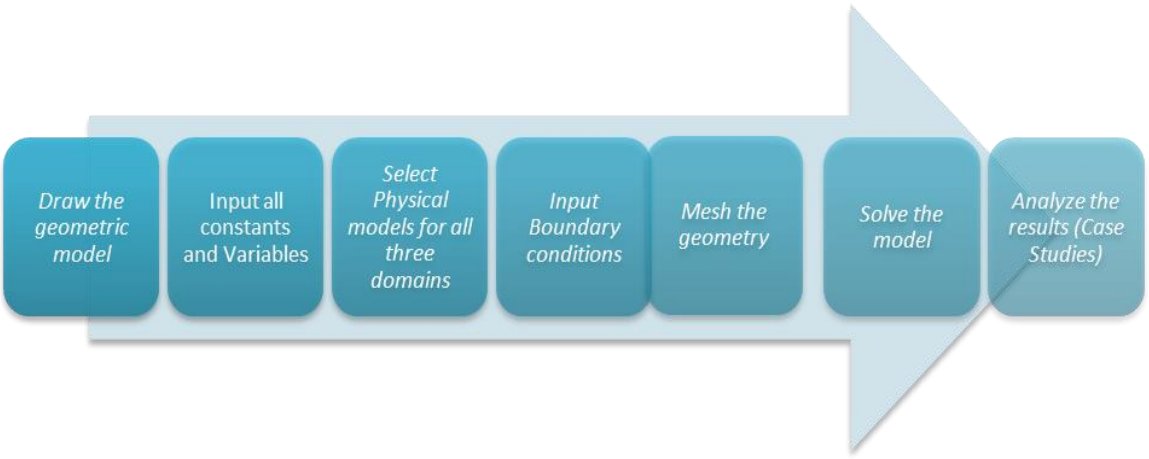

Figure 9: Steps in modelling in COMSOL

Some **assumptions** are used to chasten the model for the purpose of analysis [62].

- Flow type is Laminar as velocity is kept very low, typically less that 1m/s. Further calculations also yield that Reynolds number is less than 2100.
- Steady state operation is assumed.

- Membrane is fully hydrophobic and salt rejection is 100%.
- Losses of heat of any type to environment are ignored at all temperatures.

3.3.3.1 Step-1:-Geometric model

It consists of three regions. Left side region is feed channel, middle region is hydrophobic membrane and right side region is permeate one.

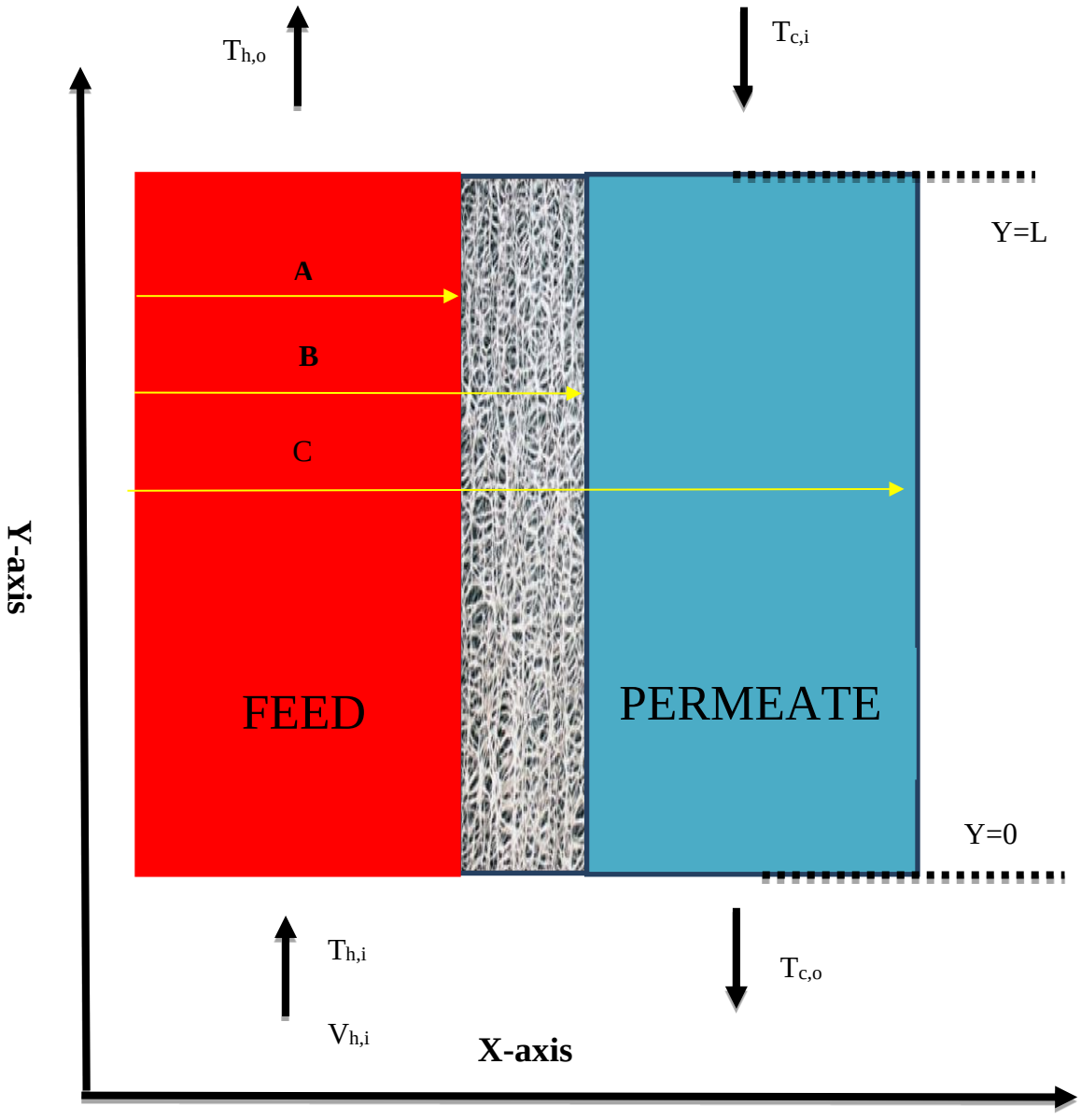

Figure 10: Geometric model in COMSOL

The value of constants are tabulated in the form of table which are given below

Table 1: Geometric parameters

Parameters	Values	Units
A	0.001	m
B	0.001145	m
C	0.0021	m
L	0.4	m

3.3.3.2 Step-2:-Constants and Variables

Here is a list of all Constants and Variables that are used in **COMSOL 5.0** for the simulation purpose.

Table 2: Constants and Variables used in COMSOL 5.0

Property	Symbol	Value	Units
CONSTANTS			
Thermal conductivity	*k_m*	0.259	*W/(m.K)*
Membrane Area	*A*	0.0300	m^2
Liquid Entry Pressure	*LEP*	100	*kPa*
Contact Angle	*CA*	132	*Degree* (^{0})
thickness	*tck*	145e-06	*M*
Pore diameter	*d*	0.22e-06	*M*
Molar mass	*M*	18.02e-03	*Moles*
Porosity	*e*	0.85	
Feed velocity	*uf*	0.5	*m/s*
Permeate velocity	*up*	0.5	*m/s*
Dynamic viscosity of feed water	*mew_f*	0.5470e-03	*Pa/s*

Dynamic viscosity of permeate water	*mew_p*	0.8900e-03	*Pa/s*
Specific heat capacity of feed water	*Cp_f*	4182	*J/(K.kg)*
Specific heat capacity of permeate water	*Cp_p*	4182	*J/(K.kg)*
Thermal conductivity of feed water	*k_f*	0.64	*W/(m.K)*
Thermal conductivity of permeate water	*k_p*	0.59	*W/(m.K)*
Density of feed water	*den_f*	988	Kg/m^3
Density of permeate water	*den_p*	997.1	Kg/m^3
Length of membrane	*L*	0.4	*M*
Gas constant	*R*	461.5	*J/(K.kg)*
VARIABLES			
Pressure at bulk feed	*P_bf*	exp(23.328-3841/(T_bf-45))	*Pa*
Pressure at bulk permeate	*P_bp*	exp(23.328-3841/(T_bp-45))	*Pa*
Tortuosity	*tur*	((2-e)^2)/e	
Heat transfer coefficient	*h_m*	k_m/tck	$(W/m^2.K)$
Heat of vaporization	*Hv*	(1.7535*(T)+2024.3)*1000	*J/kg*
Average pressure	*P_a*	(P_bf+P_bp)/2	*Pa*
Diffusion coefficient	*P_d*	(1.895e-05)*((T^(2.072)))	$Pa/m^2.s$

3.3.3.3 Step-3:-Physical models

The equation that are used for this purpose are given in **Appendix 8** are [62]:

Table 3: Physical models chosen in COMSOL 5.0

Domain	Physical model
Feed	Heat transfer in fluids (*ht*)
	Laminar flow (*spf*)
Membrane	Transport of Diluted species (*tds*)
	Heat transfer in Porous media (*ht3*)
Permeate	Heat transfer in fluids (*ht2*)
	Laminar flow (*spf2*)

3.3.3.3.1 Heat transfer in fluids

This type of model is used to accumulate and justify heat transfer in any type of region.. The heat that is transferred by conduction and convection are controlled using constants and variables that are indexed in the next section.

3.3.3.3.2 Laminar flow

It is used to represent mass or flow transfer in any region. This group of model is applied at the places where the mass transfer or flow transfer is in the laminar region i.e. its Reynolds number is less than 2100. It is applied in both feed and permeate.

3.3.3.3.3 Transport of diluted species

It is used in places where there is need for the computation of concentration field of a dilute solute in a solvent. The driving force for these type of models in diffusion. It is applied only in membrane section.

3.3.3.3.4 Heat transfer in porous media

This type of model is used for modelling heat transfer by conduction, convection and radiation in porous media. The controlling parameter for this physical model is porosity.

3.3.3.4 Step-4:-Boundary conditions

The equation that are used for this purpose are given in **Appendix 8** [63].

Table 4: Boundary conditions for feed, membrane and permeate domains in COMSOL 5.0

Location	Property	Type of condition	Equation
FEED			
x=0	Temperature	Thermal insulation	$\frac{\partial T_h}{\partial x} = 0$
	Velocity	No slip condition	$V_{X(0)} = 0$
x=A	Temperature	Equality	$T_h = T_{membrane}$
	Velocity	No slip condition	$V_{X(A)} = 0$
y=0	Temperature	Equality	$T_h = T_{h0}$
	Velocity	Equality	$V_{Y(h)} = V_{0h}$
y=L	Flux	Convection coefficient	h=h_{feed}
	Pressure	Equality	$p = p_{atm}$
MEMBRANE			
x=A	Temperature	Equality	$T_m = T_h$
	Concentration	Equality	$C = C_h$
x=B	Temperature	Equality	$T_m = T_c$
	Concentration	Equality	$C = C_c$
y=0	Temperature	Thermal Insulation	$\frac{\partial T_h}{\partial x} = 0$
	Concentration	Insulation	$\frac{\partial C_m}{\partial r} = 0$

y=L	Temperature	Thermal Insulation	$\frac{\partial T_h}{\partial x} = 0$
	Concentration	Insulation	$\frac{\partial C_m}{\partial r} = 0$
PERMEATE			
x=B	Temperature	Equality	$T_c = T_m$
	Velocity	No slip condition	$V_{X(B)} = 0$
x=C	Temperature	Thermal Insulation	$\frac{\partial T_c}{\partial x} = 0$
	Velocity	No slip condition	$V_{X(C)} = 0$
y=0	Flux	Convection coefficient	h=$h_{permeate}$
	Pressure	Equality	$p = p_{atm}$
y=L	Temperature	Equality	$T_c = T_{c0}$
	Velocity	Equality	$V_{Y(c)} = V_{0c}$

3.3.3.5 Step-5:-Mesh the Geometry

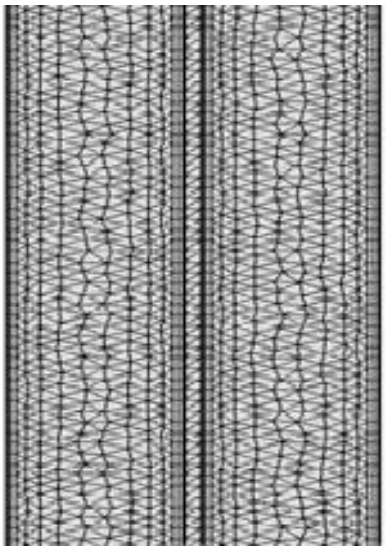

Figure 11: Mesh (Fine type)

3.3.3.6 Step-6:-Solve the model

Compute the model by clicking on “compute”. The basic gist of the things happening is the PDEs converted into set of algebraic differential equations which are solved simultaneously using boundary conditions.

3.3.3.7 Step-7:-Analyze the results (Case studies)

The last step is to analyze and study the result extensively. This is done in the form of parametric analysis in which results are studied with the help of variation of parameters. It is shown in the following flow chart

Figure 13: Process flow diagram for Analyze the Results

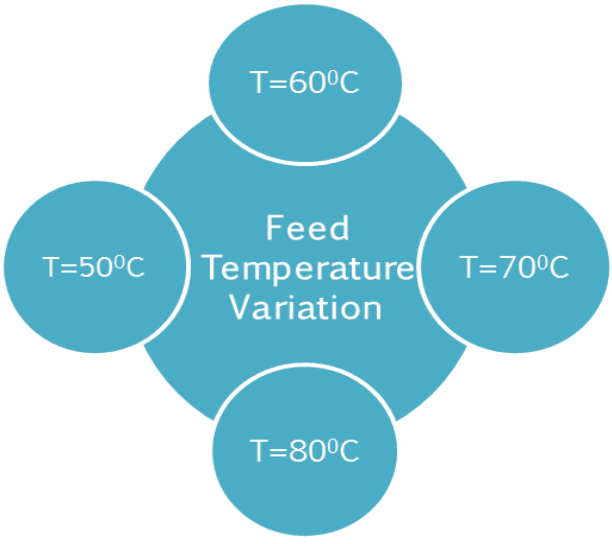

Figure 12: Case study 1- Temperature Variation

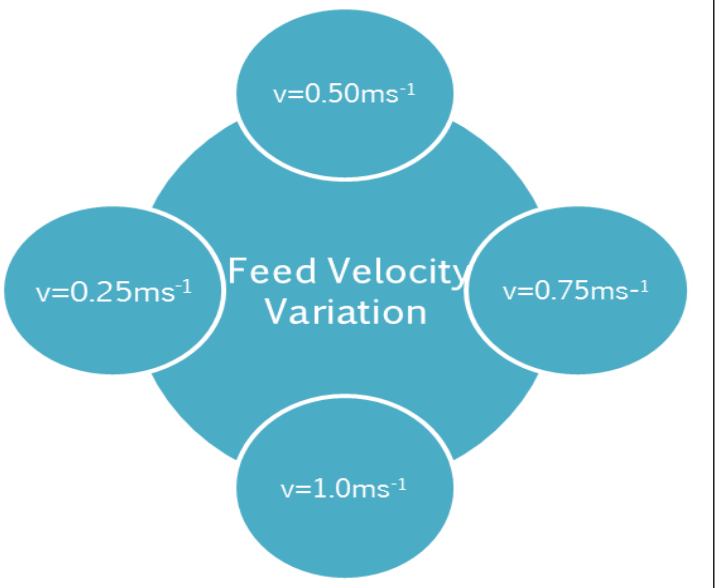

Figure 14: Case study 2- Velocity Variation

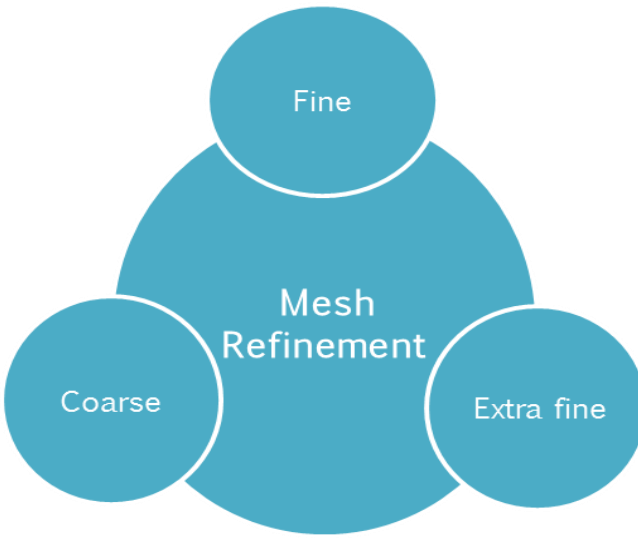

Figure 15: Case study 3- Mesh Refinement

3.4 EXPERIMENTAL DESIGN

The experimental design has been shown below. The basis of the experimental design is same as it has been described already. Hot water from the solar water heater, having steam yielded at the appropriate temperature in it comes into the feed tank and is circulated in one loop. Cold water is circulated in the other loop. This steam, when migrates from the hot side to the cold side, mixes with the cold water thus producing the clean potable water free from any salt. This system also utilizes the heat exchange particularly to employ and make use of latent heat of condensation.

Figure 16: Experimental model

Here, the red and the blue color depict the hot and the cold water in the system.

3.4.1 Major items and equipments in system

- **Membrane module**

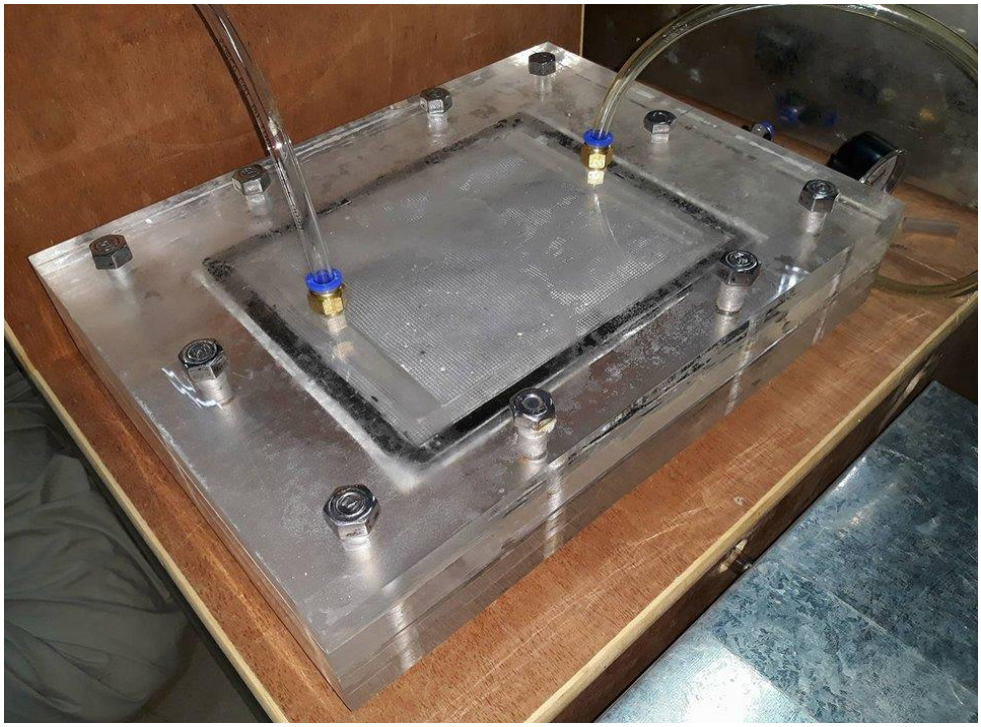

Figure 17:Membrane module

- **Tanks**

  Tanks are made up of steel. We have used 2 tanks. One as a feed tank in which hot water from solar collector comes in and one as a permeate tank in which cold water is circulated.

- **Heat exchanger**

  The heat exchanger has been employed in this system particularly to make use of the latent heat of condensation. The heat exchanger type is the box and tube heat exchanger. The total number of tubes that are employed are 12, the calculations of which are given in the calculations section.

Figure 18: Heat exchanger

- **Solar water heater**

  We didn't purchase the solar water heater. We did our experimentation with the one placed on the top of the roof at DME. It was an evacuated solar water heater.

Figure 19: Solar water heater

- **Plastic pipes**

  Plastic pipes of variety of sizes were used to fulfill the requirement of flow of water from one part to another.

Figure 20: Pipes

- **Fittings**

  Different types of fittings like tee joint, nuts, connectors were also used.

Figure 21: Connectors

Figure 22: Tee joint

- **Thermocouple**

  The thermocouple used was of MAX 6675. It was a K type thermocouple. It was a 5 pin temperature sensor which can measure the temperature in the range of -20^{o}C to 120^{o}C with a resolution of 0.25^{o}C. The voltage required for this type of thermocouple was 5V.

Figure 23: Thermocouple

- **Pressure gauge**

  The pressure gauge that was employed can measure in the range of 0 to 10 psi.

Figure 24: Thermocouple

- **Water flow sensor**

  The 3 pin water flow sensor was of Hall Effect type sensor. It was operated on 5V and had a capacity in the range of 1L/min to 12L/min.

Figure 25: Flow sensor

- **Electrical components**

  Many electrical components were used that made our system more advanced.

  1. Arduino UNO
  2. Wires (Male to Male, Male to female, Female to Female)
  3. Breadboard
  4. LCD (16*4)

Figure 27: Arduino

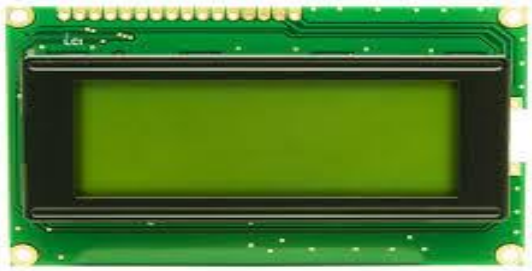

Figure 26: LCD

3.5 EXPERIMENTAL CALCULATIONS

According to the insights of our experiments, we designed the heat exchanger and found out the number of tubes that are used in making of box and tube heat exchanger. The calculations are based on LMTD method as follows:

Hot Fluid

$T_1 = 60\ ℃ = 333\ K$

$T_2 = 45\ ℃ = 318\ K$

Cold Fluid

$t_1 = 30\ ℃ = 303\ K$

$t_2 = 40\ ℃ = 313\ K$

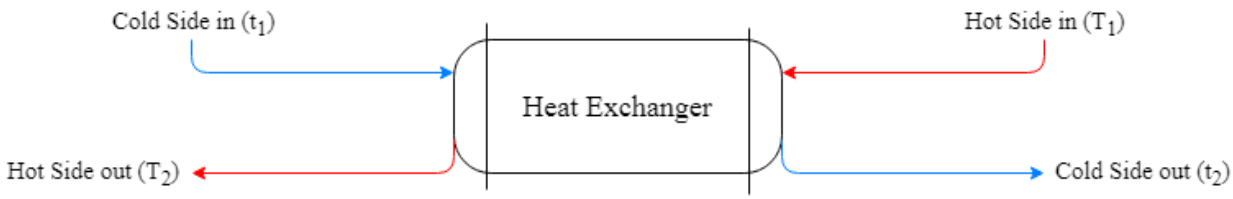

Figure 28: Heat transfer across HX

Overall heat transfer coefficient $= U = 455\ Wm^{-2}K^{-1}$

Mass flow rate of water $= \dot{m} = 10\ Lm^{-1} = 0.167\ kgs^{-1}$

The required heat transfer rate is $= \dot{Q} = \dot{m}C_p\Delta T = 0.167 \times 4.18 \times 10^3 \times (333 - 318)$

$$= 7470.9\ W = 7.471\ kW$$

Log Mean Temperature Difference (LMTD) is given by:

$$\Delta T_m = \frac{(T_1 - t_2) - (T_2 - t_1)}{ln\frac{(T_1 - t_2)}{(T_2 - t_1)}}$$

$$\Delta T_m = \frac{(333 - 313) - (318 - 303)}{ln\frac{(333 - 313)}{(318 - 303)}}$$

$$\Delta T_m = 24.38\ K$$

The area of heat exchanger can now be calculated as:

$$A = \frac{\dot{Q}}{U \times \Delta T_m}$$

$$A = \frac{7470.9}{455 \times 24.38}$$

$$A = 0.573\ m^2$$

The required mass flow rate can be determined from:

$$\dot{m} = \frac{\dot{Q}}{C_p \Delta T_m}$$

$$\dot{m} = \frac{7470.9}{4.18 \times 10^3 \times 24.38}$$

$$\dot{m} = 0.144\ kgs^{-1}$$

Now Tube length $= L = 1.5\ ft$

Tube diameter $= D = 1\ in$

So surface area per tube will be:

$$S_a = \pi DL$$

$$S_a = \pi\left(\frac{1}{12}\right)(1.5)$$

$$S_a = 0.393\ ft^2$$

Thus the number of tubes required is:

$$n = \frac{A}{S_a}$$

$$n = \frac{0.573\ m^2}{0.393\ ft^2}$$

$$n = \frac{6.168\ ft^2}{0.393\ ft^2}$$

$$\boldsymbol{n = 15.69\ tubes\ (16\ tubes)}$$

CHAPTER 4: RESULTS AND DISCUSSIONS

4.1 RESULTS OF MATLAB FOR MEMBRANE DISTILLATION

The results in the Matlab are generated with reference of the code from the MATLAB. The codes are based on the system of iterative scheme and calculate the flux on the basis of temperatures such that different between temperatures is less than tolerance.

Various characteristics of module are analyzed to ensure the optimum properties that can be used in our practical model. The properties like porosity, feed bulk temperature etc. are varied to see their effect on the water flux which depend on the difference of temperature on both sides of membrane. These results are shown below:

4.1.1 Effect of Porosity of membrane on Mass flux

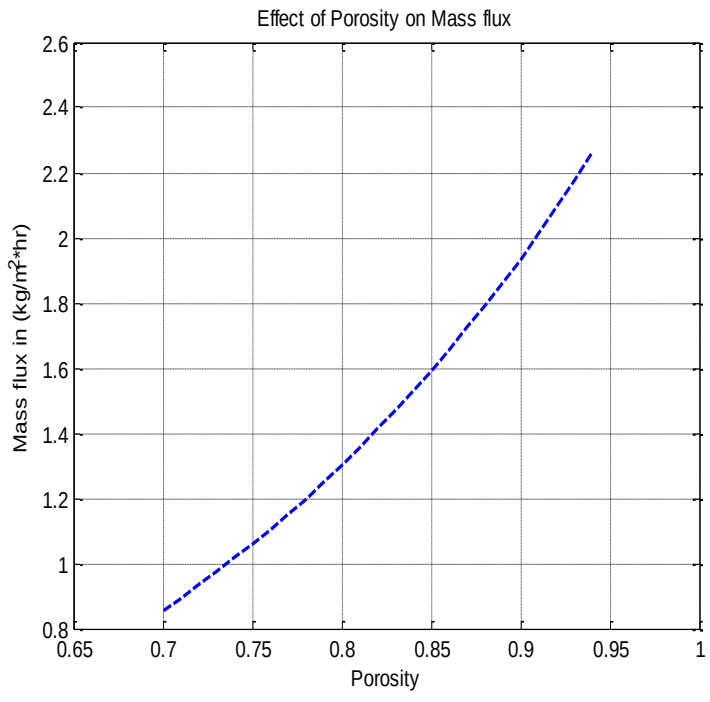

Data

Feed Temperature = 333K

Permeate Temperature = 293K

Feed velocity = 0.5m/s

Permeate velocity = 0.5m/s

Thickness = 145e-06m

Thermal conductivity= 0.259 W/ (m.K)

Area = 0.0300m^2

Pore diameter = 0.22e-06m

Figure 29: Effect of Porosity of membrane on Mass flux

Results of Matlab irrefutably show that increase in the porosity of membrane from 0.7 to 0.94 directly enhances the value of Permeate flux from 0.87kg/m^2hr to 2.27kg/m^2hr. Basically porosity is the fraction of voids present in the material. So if the porosity is 75%, it means that 3 quarters of the material has spaces inside it out of 4 quarters and only 1 quarter has solid material.

As the porosity is increased, percentage of voids in membranes gets amplified which results in additional amount of vapors passing through it [10] . This enhanced vapors then condenses on the permeate side to yield more mass flux in terms of clean potable water. It is specifically important to mention that pore diameter also affects the porosity but it cannot be greater than the size of water molecule as then it will not be able to block the water molecule and surface tension forces will fall short of it.

4.1.2 Effect of feed Temperature on Mass flux

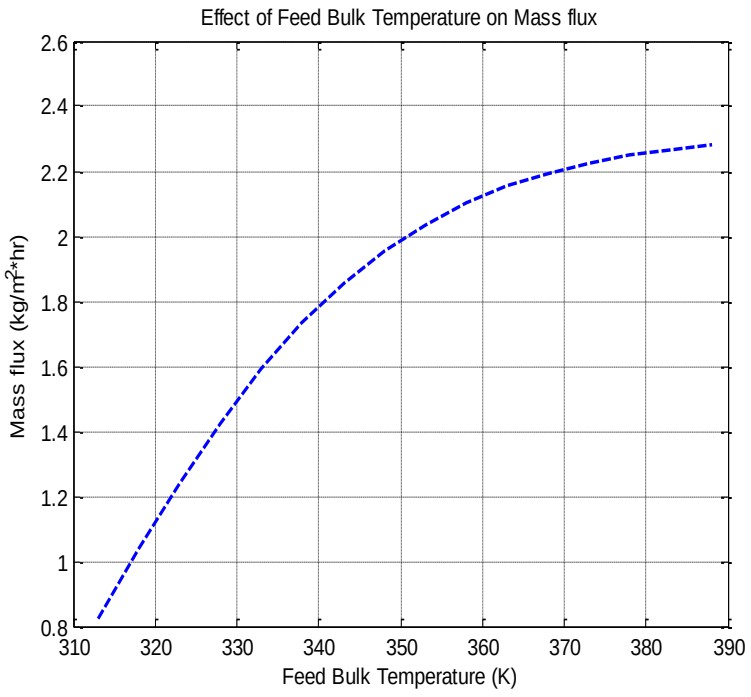

Data

Permeate Temperature = 293K

Feed velocity = 0.5m/s

Permeate velocity = 0.5m/s

Thickness = 145e-06m

Porosity = 0.85

Thermal conductivity= 0.259 W/ (m.K)

Area = 0.0300m^2

Pore diameter= 0.22e-06m

Figure 30: Effect of feed Temperature on Mass flux

Bulk feed temperature is the temperature of the water on the feed side and is controlled by solar collector in our case. The temperature control in solar collector is primarily dependent on the extent of radiation falling on it as well as its efficiency. As inferred from the graph above, enhancement in feed temperature intensified the permeate flux. The reason is that escalation of Bulk feed temperature raises the temperature difference across the membrane due to which pressure difference is increased across both sides according to Antione equation,

$$J_w = B_m(P_{mf} - P_{mp})$$

Also when the feed temperature is increased, the temperature of the vapors moving across permeate side is also high which gives it more proportion to get condensed in a proper way as compared to low temperature. The results are very close to [28] with error quite less than 10%.

4.1.3 Effect of feed velocity on Mass flux

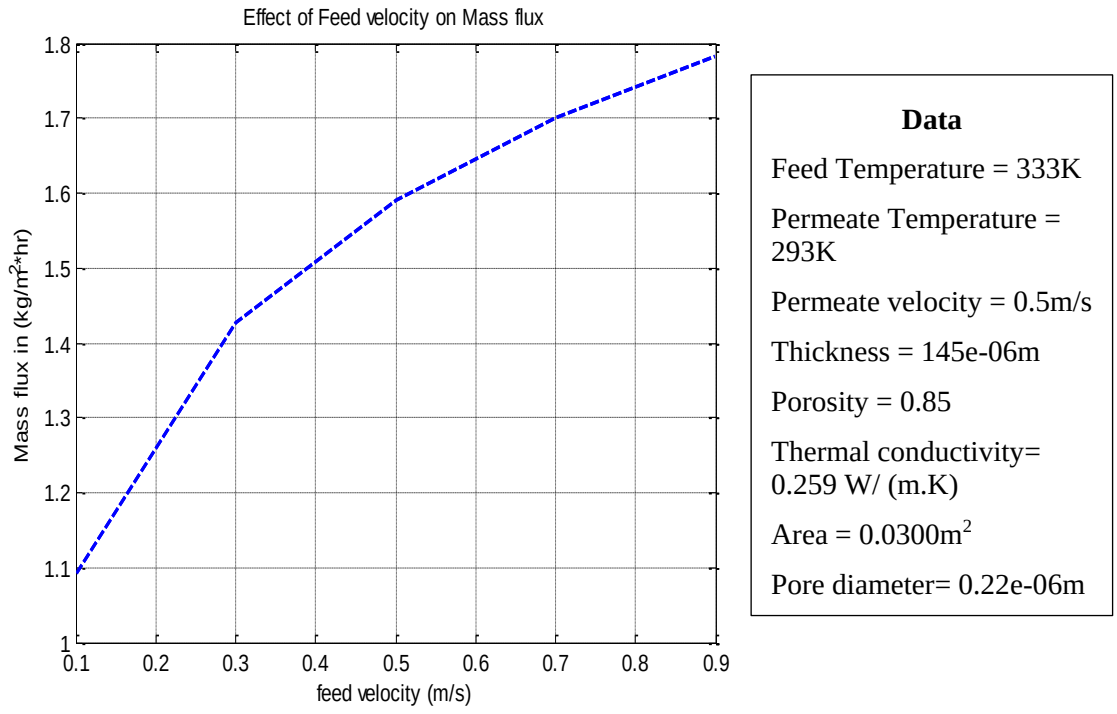

Figure 31: Effect of feed velocity on Mass flux

The results are quite close to [28] for feed velocity with error less than 10%.. It is the average velocity of the water entering the feed side and exiting it. Raising the velocity of feed water from 0.1m/s to 1m/s amplifies the flux from 1.09kg/m^2hr to 1.78kg/m^2hr. The factor that is responsible for this is increase in Reynolds number. This makes it close to turbulent nature of water which results in high rate of mixing and effective heat transfer.

$$Re = pvd/\ \mu$$

Another reason that accounts for this is that turbulent flow has heat transfer in azimuthal and radial directions which is termed as "**Eddy transport**" [64].This does not happen in laminar flow where conduction is the dominating phenomenon only.

4.1.4 Effect of thickness on Mass flux

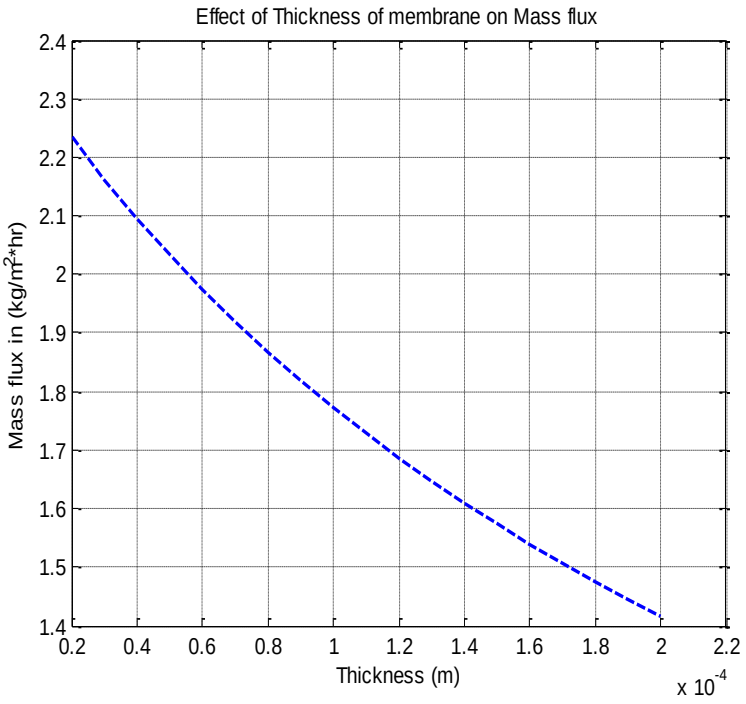

Data

Feed Temperature = 333K

Permeate Temperature = 293K

Feed velocity = 0.5m/s

Permeate velocity = 0.5m/s

Porosity = 0.85

Thermal conductivity= 0.259 W/ (m.K)

Area = 0.0300m^2

Pore diameter = 0.22e-06m

Figure 32: Effect of thickness on Mass flux

Effect of thickness on flux has been shown in the above graph.. It is clearly exhibited that flux is quite sensitive to thickness and increase in the thickness of membrane decreases the Water flux. When the membrane is thin, heat that will be transferred by conduction will be excessive that's leads to low heat efficiency of this process [65]. But it is very important to mention here that optimum conditions are very important to have greater mass flux and compromise should be made between heat and mass transfer by adjusting its thickness. It is also governed by [10]:

$$N \propto \varepsilon r^{a}/\tau\delta$$

Where N is the molar flux passing through membrane and δ is thickness of hydrophobic membrane.

Above relation clearly shows that membrane thickness is inversely proportional to the Permeate flux and it increases as thickness is decreased.

4.2 RESULTS OF MATLAB FOR SOLAR COLLECTOR

The results in the Matlab for the solar collector are generated with reference of the code which is given in the Appendix **7**. This code is typically based on the system of iterative scheme until the solution converges based on the criteria we set in the code. The results are generated according to the conditions mentioned in the document with some variations where necessary [61].

Initial temperature of water in the tank = 20^{o}C

Number of nodes along the tube of solar collector =8

Volume of the tank in liters = 3m^{3}

Flow rate entering into the system in GPM (Galloon per minute) = 1.7 GPM

Average Solar flux = 295 W/m^{2} [66]

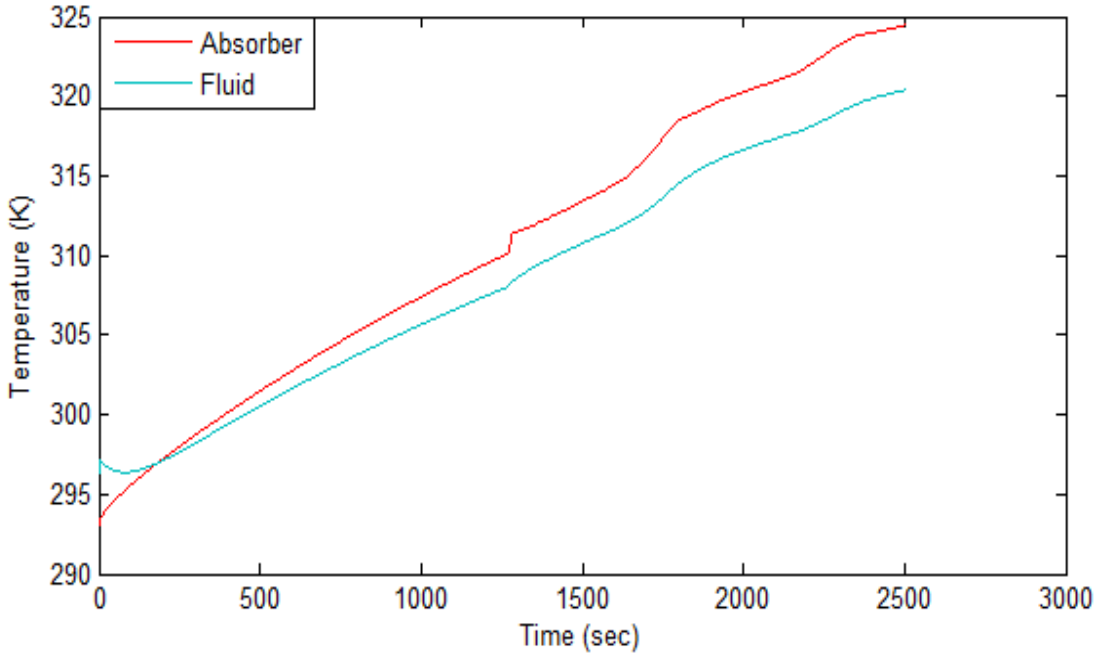

Figure 33: Time vs Temperature of Solar collector

4.2.1 Discussion

By looking at the graph, we can see that the temperature of the fluid in the tank has reached up to 47.2^0C. This is quite close to the results of [61] where on the basis of above mentioned conditions, temperature has been reached up to 50^oC. Also due to the losses occurring to the environment during the transfer of heat from absorber to the fluid circulating in the pipes, fluid has not been able to reach the temperature of absorber.

These results are generated on the basis of nominal conditions. However, in practical, the temperature of the circulating fluid could get higher with reference to the increment in the properties like average solar flux, flow rate of the fluid entering into the system etc.

4.3 RESULTS OF SIMULATIONS IN COMSOL

The results are scrutinized and compared with various research paper results. Three different group of results are inspected extensively for different values.

- Bulk feed Temperature
- Bulk feed velocity
- Mesh refinement

4.3.1 TEMPERATURE Variation

We have used the following properties and compared with [28, 57]

Feed velocity=uf=0.5m/s **Permeate velocity=up=0.5m/s**

4.3.1.1 Temperature = 50K

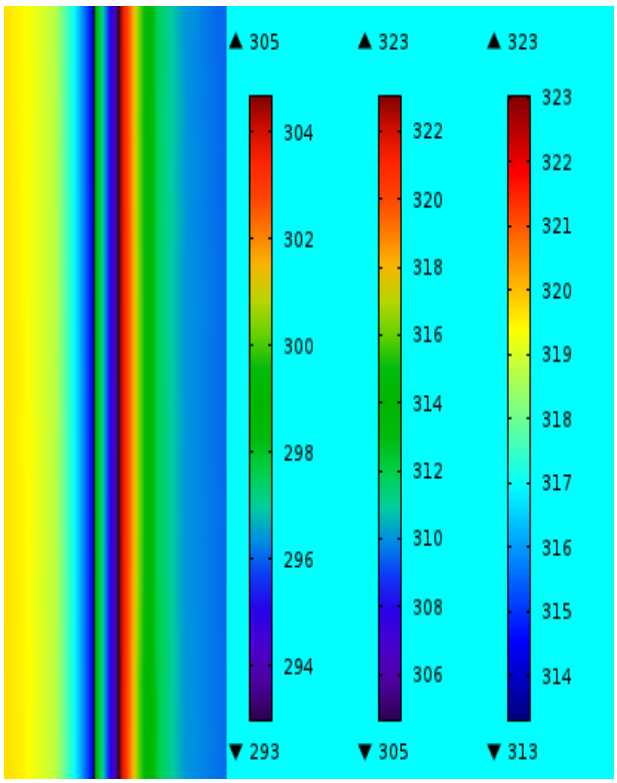

Figure 35: Temperature contour (50K)

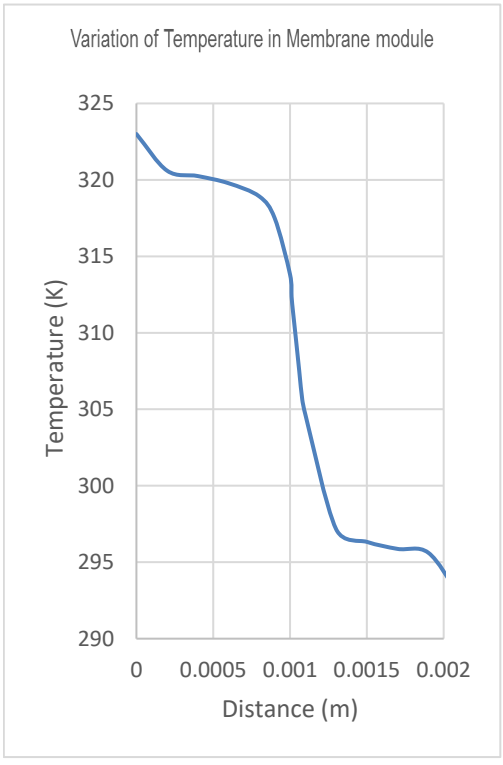

Figure 34: Flux vs. Temperature (50K)

Table 5: Flux comparison in COMSOL and MATLAB for Tbf=323K

Software	Feed temperature (T_{bf}) (K)	Permeate Temperature (T_{bp}) (K)	Membrane Feed temperature (T_{mf}) (K)	Membrane permeate temperature (T_{mp}) (K)	Permeability constant (B)	Flux (J) [28, 57] kg/m^2.hr
COMSOL	323	293	313.97	304.65	1.06e-07	1.19
MATLAB	323	293	313.33	303.24	1.06e-07	1.24

The difference in flux is particularly due to difference in Temperature as Temperature difference dictates Pressure difference which affects the flux by Antoine equation [14].

$$J = B(P_{mf-} P_{mp})$$

Where $$P = \exp(23.328 - \frac{3841}{T-45})$$

4.3.1.2 Temperature = 60K

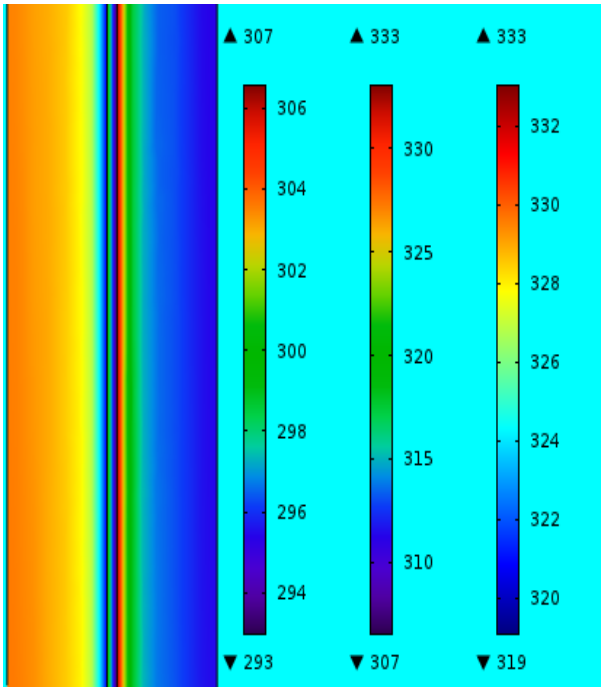

Figure 36:Temperature contour (60K)

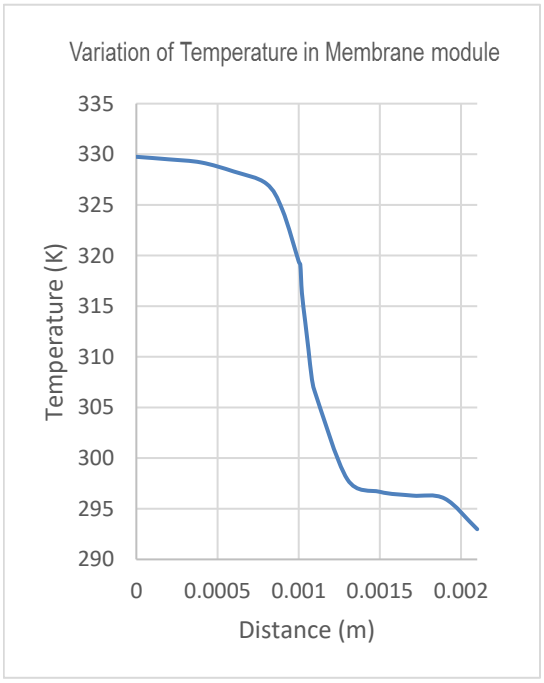

Figure 37: Flux vs. Temperature (60K)

Table 6: Flux comparison in COMSOL and MATLAB for Tbf=333K

Software	Feed temperature (T_{bf}) (K)	Permeate Temperature (T_{bp}) (K)	Membrane Feed temperature (T_{mf}) (K)	Membrane permeate temperature (T_{mp}) (K)	Permeability constant (B)	Flux (J) [28, 57] kg/m^2.hr
COMSOL	333	293	319.62	306.42	8.03e-08	1.53
MATLAB	333	293	320.11	306.53	8.03e-08	1.59

Difference in flux is due to difference in Temperature as Temperature difference refers to Pressure difference which affects the flux by the following equation [14]:

$$J = B(P_{mf-} P_{mp})$$

Where $$P = \exp(23.328 - \frac{3841}{T-45})$$

4.3.1.3 Temperature = 70K:

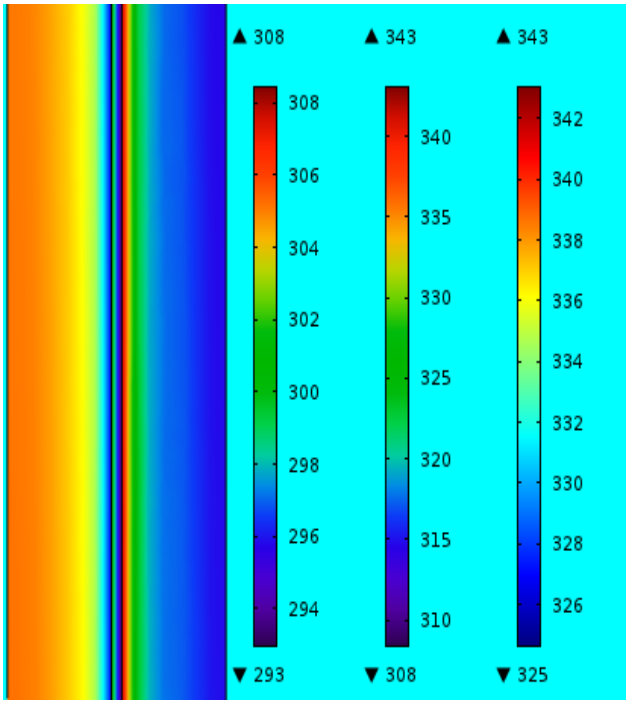

Figure 39:Temperature contour (70K)

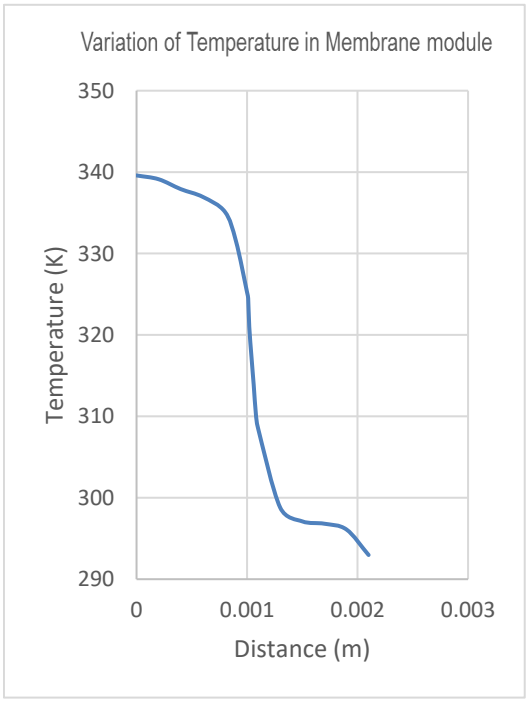

Figure 38: Flux vs. Temperature (70K)

Table 7: Flux comparison in COMSOL and MATLAB for Tbf=343K

Software	Feed temperature (T_{bf}) (K)	Permeate Temperature (T_{bp}) (K)	Membrane Feed temperature (T_{mf}) (K)	Membrane permeate temperature (T_{mp}) (K)	Permeability constant (B)	Flux (J) [28, 57] kg/m^2.hr
COMSOL	343	293	325.693	308.52	5.91e-08	1.77
MATLAB	343	293	326.90	309.94	5.91e-08	1.85

The difference in flux is due to difference in Temperature as Temperature difference dictates Pressure difference which affects the flux by the equation as follows [14]:

$$J = B(P_{mf-} P_{mp})$$

Where $$P = \exp(23.328 - \frac{3841}{T-45})$$

4.3.1.4 Temperature = 80K:

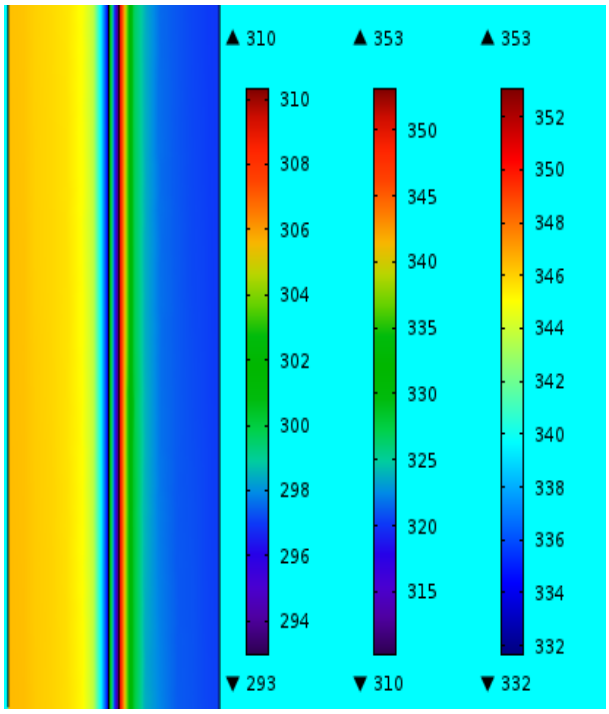

Figure 41:Temperature contour (80K)

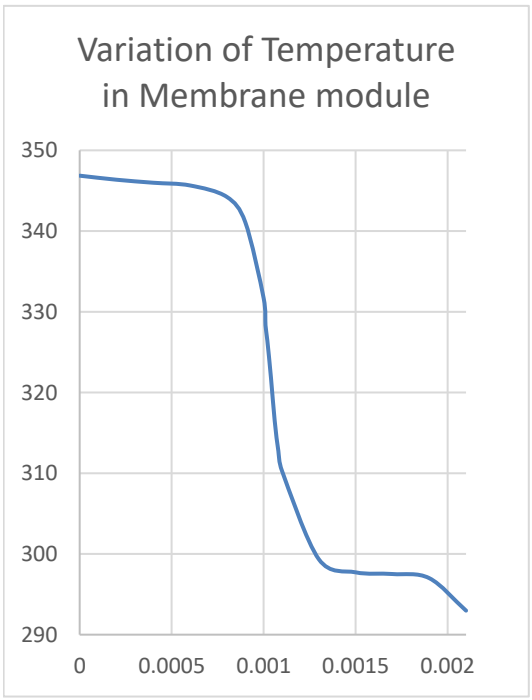

Figure 40: Flux vs. Temperature (80K)

Table 8: Flux comparison in COMSOL and MATLAB for Tbf=353K

Software	Feed temperature (T_{bf}) (K)	Permeate Temperature (T_{bp}) (K)	Membrane Feed temperature (T_{mf}) (K)	Membrane permeate temperature (T_{mp}) (K)	Permeability constant (B)	Flux (J) [28, 57] kg/m^2.hr
COMSOL	353	293	331.78	308.52	4.31e-08	1.94
MATLAB	353	293	333.90	311.94	4.31e-08	2.03

The difference in flux is due to difference in Temperature as Temperature difference dictates Pressure difference which affects the flux by the equation as follows [14]:

$$J = B(P_{mf-} P_{mp})$$

Where $$P = \exp(23.328 - \frac{3841}{T-45})$$

4.3.1.5 Mutual graph of Membrane interfaces temperature

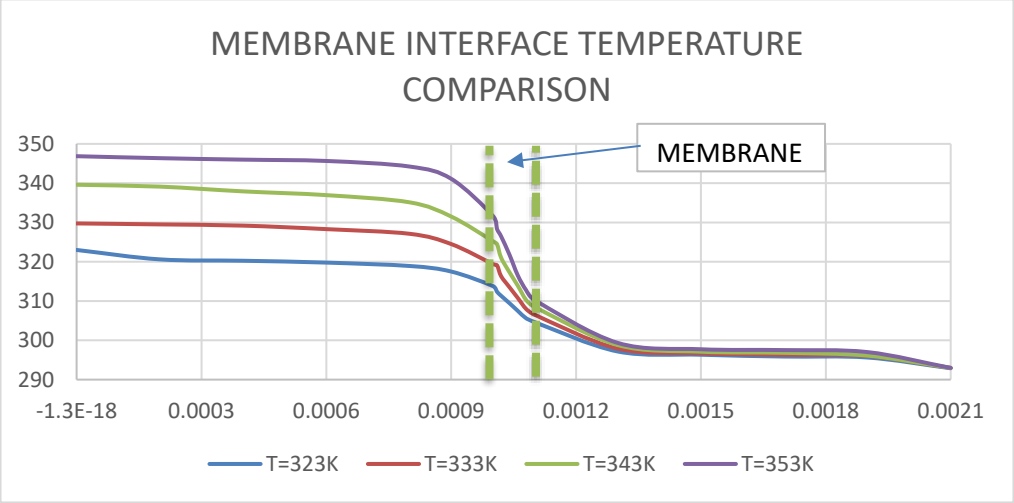

Figure 42: Comparison of Membrane Interface Temperatures at different Feed Temperatures from COMSOL

The above graph clearly show that as the feed temperature is increased, Membrane interface temperature difference also increases which causes an increase in the flux due to the increased pressure according to Antoine equation [14]. That is why, the higher the temperature, higher is the flux.

4.3.1.6 Flux Comparison

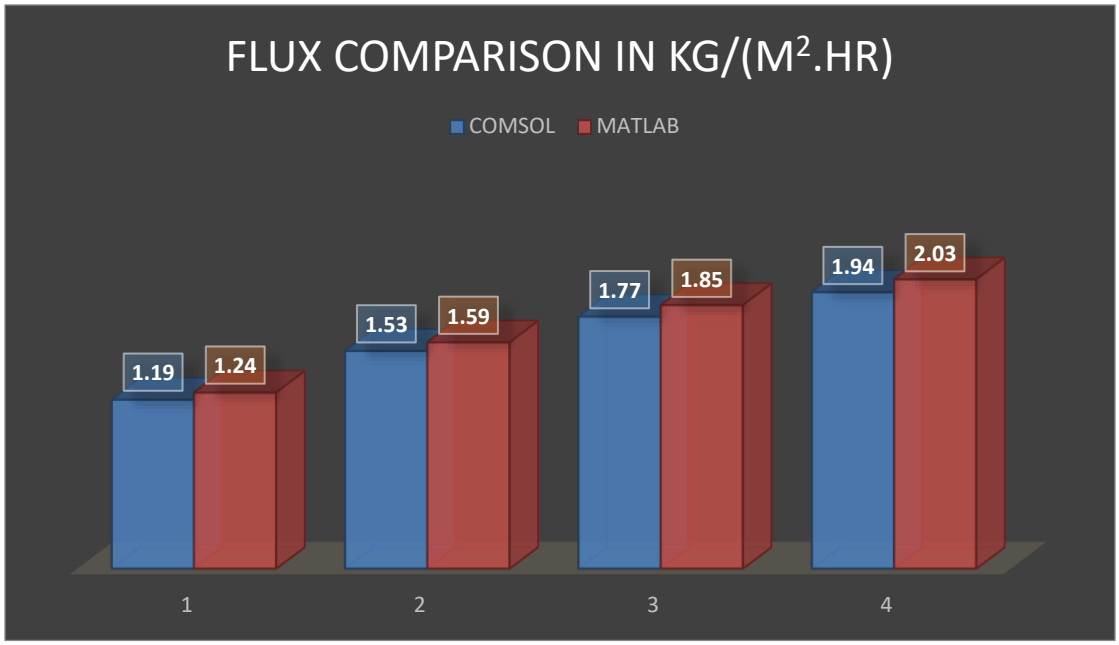

Figure 43: Flux comparison between two softwares by changing temperatures

4.3.1.6.1 Comment

From the graph (going from left to right), we can have an overview of the results from MATLAB and COMSOL both. The difference between the results for all temperature is quite less and error is less than 10%.It also infers that as the feed temperature is increased, flux continuous to increase till it reaches the steady value. This has been proved in both software's. The result of COMSOL are compared with [28, 57] with the help of techniques referred in the papers.

4.3.2 VELOCITY Variation

For variation in velocity [1], we have used the following properties [28, 57]:

Feed Bulk Temperature=T_{bf}=333K

Permeate Bulk Temperature=T_{bp}=293K

4.3.2.1 Velocity = 0.25ms^{-1}

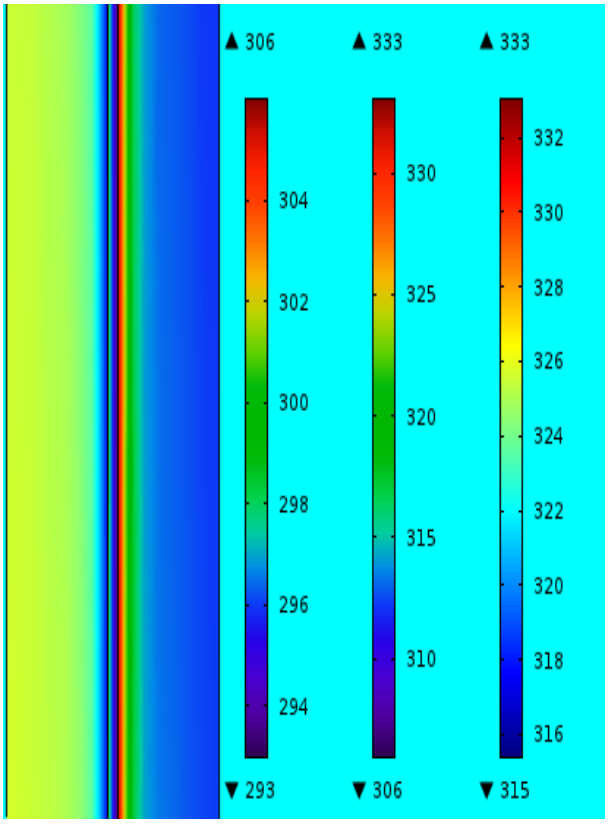

Figure 44: Velocity contour (0.25m/s)

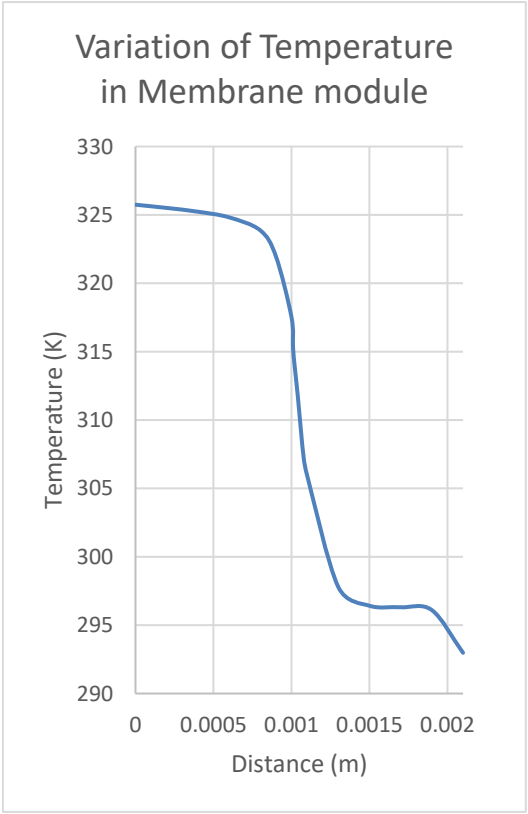

Figure 45: Flux vs. Temperature (Vel=0.25m/s)

Table 9: Flux comparison in COMSOL and MATLAB for uf=0.25m/s

Software	Feed velocity (uf) (ms^{-1})	Permeate velocity (up) (ms^{-1})	Membrane Feed temperature (T_{mf}) (K)	Membrane permeate temperature (T_{mp}) (K)	Permeability constant (B)	Flux (J) [28, 57] $kg/m^2.hr$
COMSOL	0.25	0.5	317.98	305.97	8.03e-08	1.32
MATLAB	0.25	0.5	313.33	303.24	1.06e-07	1.36

The velocity of 0.25m/s yield a very low Reynolds no as a result of which it exists at the low level of laminar region. Heat transfer in laminar region is not as effective as in turbulent region due to which heat losses incur [10, 64]. That's why the flux value is moderate.

4.3.2.2 Velocity = 0.50ms^{-1}

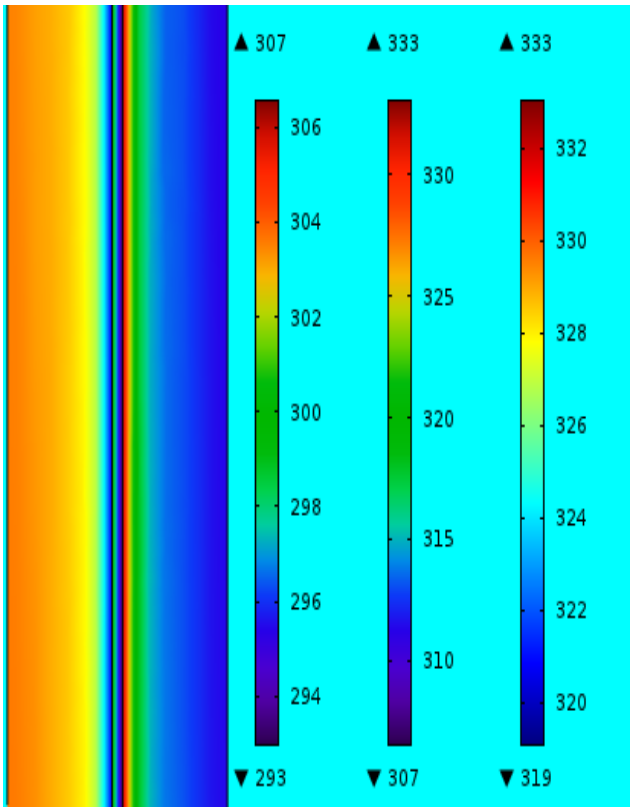

Figure 46: Velocity contour (0.5m/s)

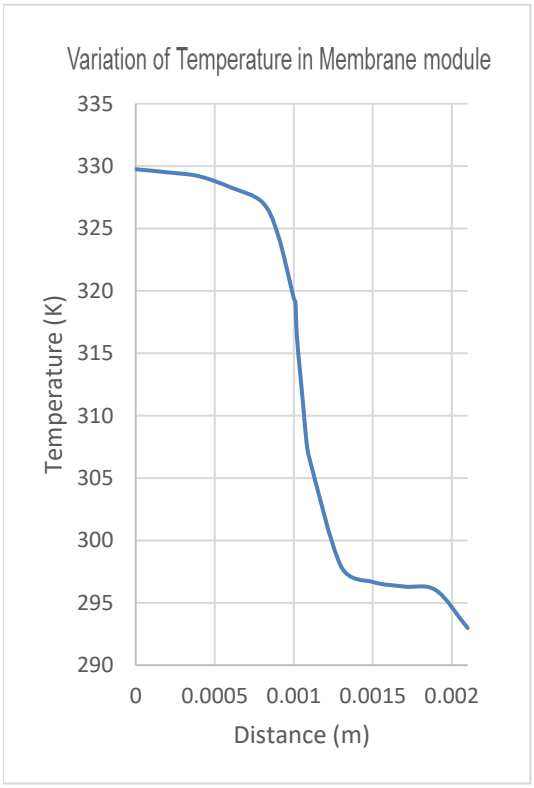

Figure 47: Flux vs. Temperature (Vel=0.5m/s)

Table 10: Flux comparison in COMSOL and MATLAB for uf=0.5m/s

Software	Feed velocity (uf) (ms^{-1})	Permeate velocity (up) (ms^{-1})	Membrane Feed temperature (T_{mf}) (K)	Membrane permeate temperature (T_{mp}) (K)	Permeability constant (B)	Flux (J) [28, 57] $kg/m^2.hr$
COMSOL	0.5	0.5	319.62	306.42	8.03e-08	1.53
MATLAB	0.5	0.5	320.11	306.53	8.03e-08	1.59

The velocity of 0.5m/s yield a low Reynolds no due to which it exists at the low level of laminar region. Heat transfer in laminar region is not as effective as in turbulent region due to which heat losses incur. That's why the flux value is nominal at this velocity [10, 64].

4.3.2.3 Velocity = 0.75ms^{-1}

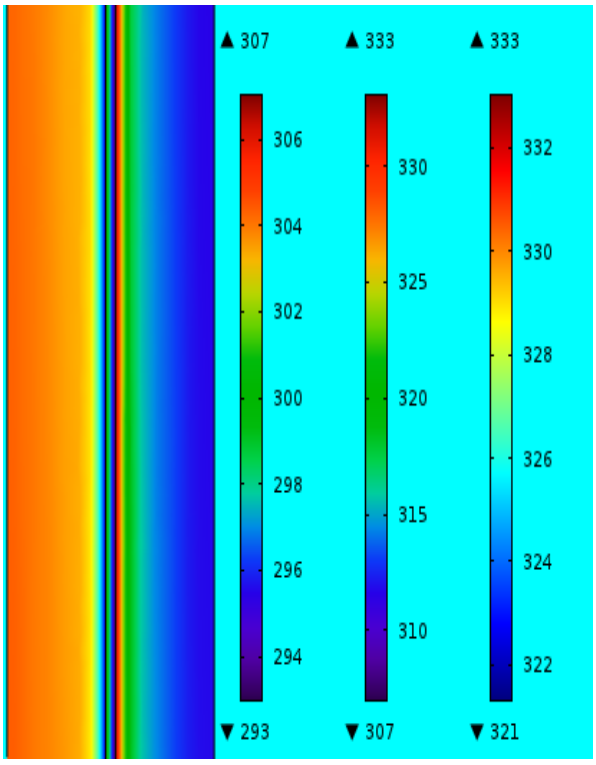

Figure 48: Velocity contour (0.75m/s)

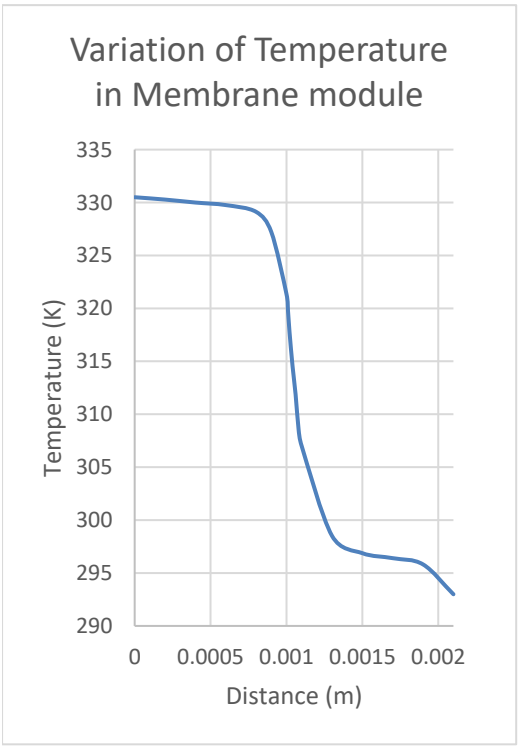

Figure 49: Flux vs. Temperature (Vel=0.75m/s)

Table 11: Flux comparison in COMSOL and MATLAB for uf=0.75m/s

Software	Feed velocity (uf) (ms^{-1})	Permeate velocity (up) (ms^{-1})	Membrane Feed temperature (T_{mf}) (K)	Membrane permeate temperature (T_{mp}) (K)	Permeability constant (B)	Flux (J) [28, 57] $kg/m^2.hr$
COMSOL	0.75	0.5	321.26	307.002	8.03e-08	1.74
MATLAB	0.75	0.5	321.24	307.14	8.03e-08	1.72

The velocity of 0.75m/s generates a low Reynolds no relatively as a result of which it exists at the low level of laminar region. Heat transfer in laminar region is not as efficient as in turbulent region. That's why the flux value is comparatively high [10, 64].

4.3.2.4 Velocity = 1.0ms^{-1}

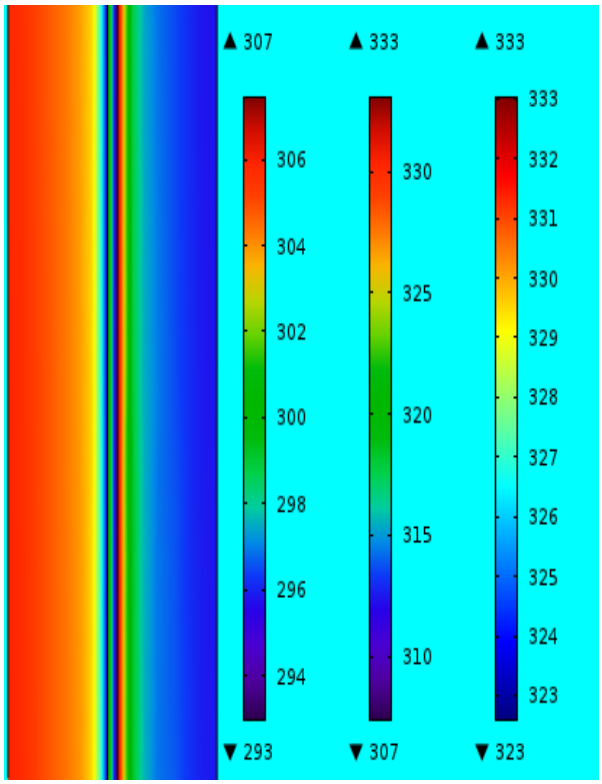

Figure 52: Velocity contour (1.0m/s)

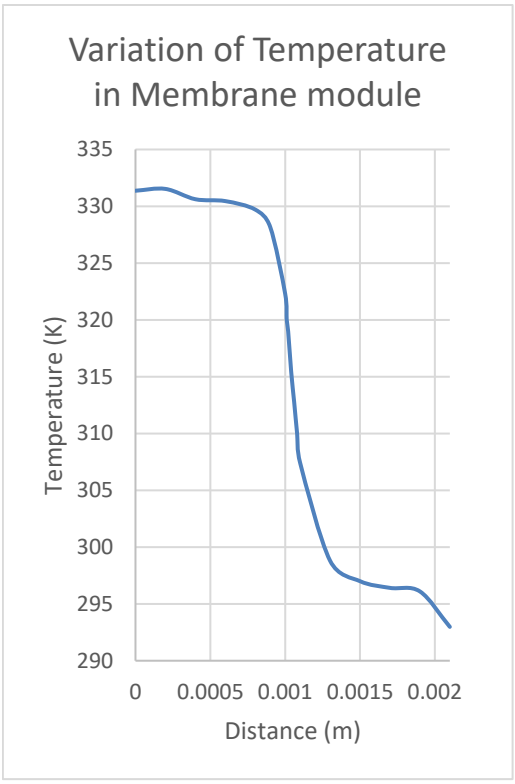

Figure 50: Flux vs. Temperature (Vel=1m/s)

Table 12: Flux comparison in COMSOL and MATLAB for uf=1.00m/s

Software	Feed velocity (uf) (ms^{-1})	Permeate velocity (up) (ms^{-1})	Membrane Feed temperature (T_{mf}) (K)	Membrane permeate temperature (T_{mp}) (K)	Permeability constant (B)	Flux (J) [28, 57] $kg/m^2.hr$
COMSOL	1.0	0.5	322.19	307.41	8.03e-08	1.85
MATLAB	1.0	0.5	322.01	307.53	8.03e-08	1.82

The velocity of 1.0m/s generates a relatively high Reynolds no. due to which it exists at the high level of laminar region. Heat transfer in laminar region becomes effective and efficient as it is approaching the turbulent behavior and thus results in high flux [10, 64].

4.3.2.5 Mutual graph of Membrane interfaces temperature

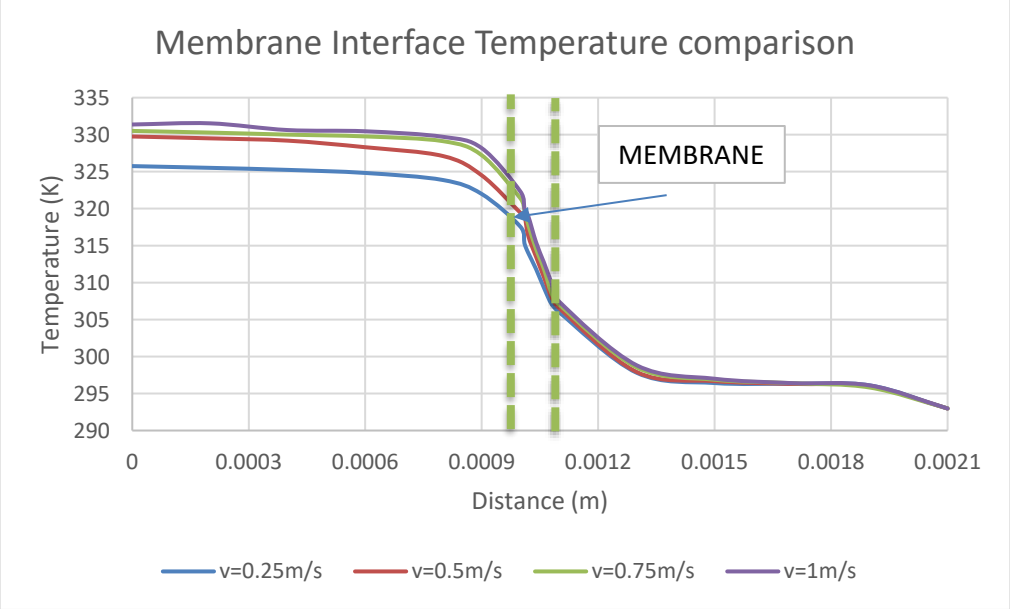

Figure 53: Comparison of Membrane Interface Temperatures at different Feed velocities from COMSOL

The above graph clearly shows that as the feed velocity is increased, flux increases from 1.32 *kg/m*^{2}*.hr* to 1.85 *kg/m*^{2}*.hr*. This is because as the velocity is enhanced from 0.25 *m/s* to 1.0 *m/s*, the nature of flow is shifting from laminar to turbulent until it becomes steady which refers to the increase in Reynolds number [10]. This makes it close to tumultuous nature of water which results in high rate of mixing. When there is rapid mixing, there is better and efficient heat transfer without prominent losses.

$$Re = \frac{pvd}{\mu}$$

Another reason that accounts for this is that turbulent flow has heat transfer in azimuthal and radial directions which is termed as "Eddy transport" [64].This does not happen in laminar flow where conduction is the dominating phenomenon only.

4.3.2.6 Flux Comparison

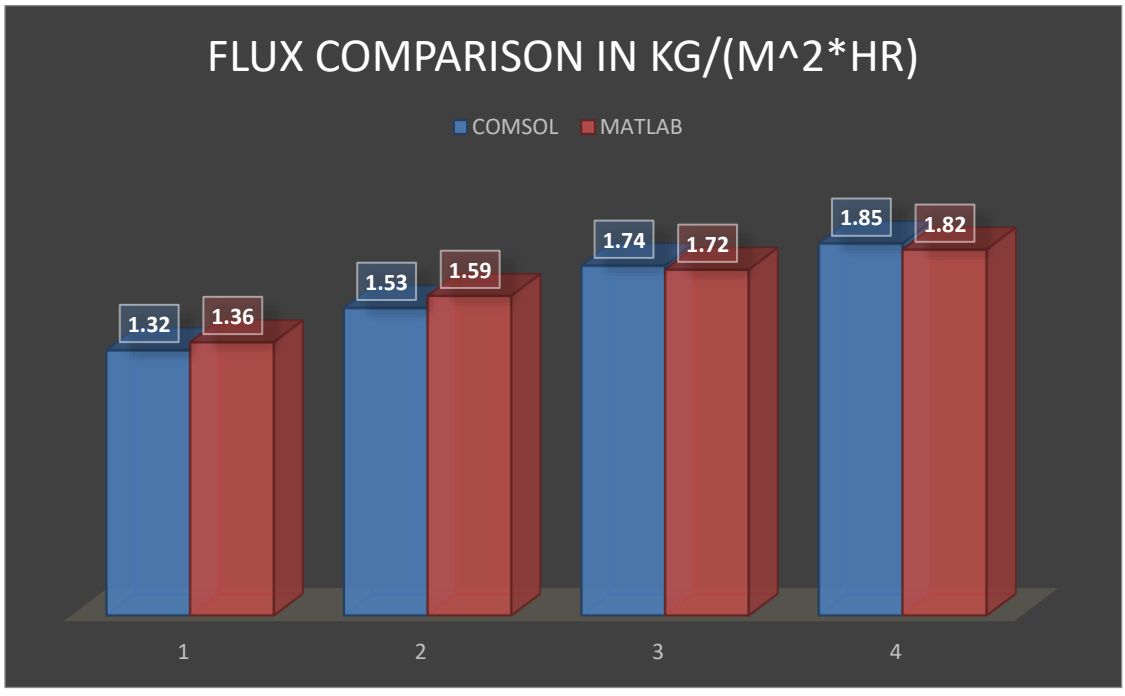

Figure 54: Flux comparison between two softwares by changing velocities

4.3.2.6.1 Comment

Variation in flux is accounted to the variation in bulk feed velocities as shown above in the figure. The difference between the results of two software's is very much less which verifies and validates the correctness of above results [28, 57]. The enhancement in flux is actually due to the increase in the feed velocities and it will continue to increase till it finally reaches the steady value.

4.3.3 MESH REFINEMENT

The third study is related to mesh refinement which means that the results are carried out with different mesh levels. Mesh refinement basically means dividing the domain or system in elements according to the quality of mesh. Results will be checked for three cases one by one:

- Coarse
- Fine
- Extra Fine

The criteria for checking the results will be that as the mesh quality is increased, results will be much closer to authentic values. Also increasing the mesh quality causes the processor of system to work more, resulting in delayed and efficient results. Also as the number of elements are enhanced, software will contain more and more equation and more work will have to be done by processor of system so mesh quality depends a lot on the processing power of system. So more quality of mesh, more will be burden on system to yield the results.

For example, a coarse mesh will have require very less computational power to generate the results but on the other hand, if we talk about fine mesh, it will need more processing power because the mesh will be much more refined and number of elements will be much greater as compared to the coarse mesh case.

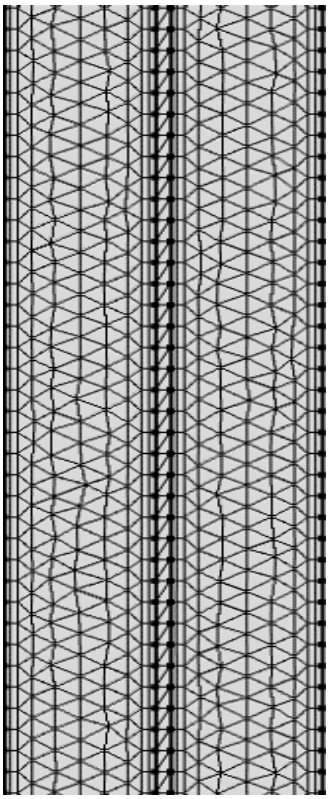

Figure 57: Coarse Mesh

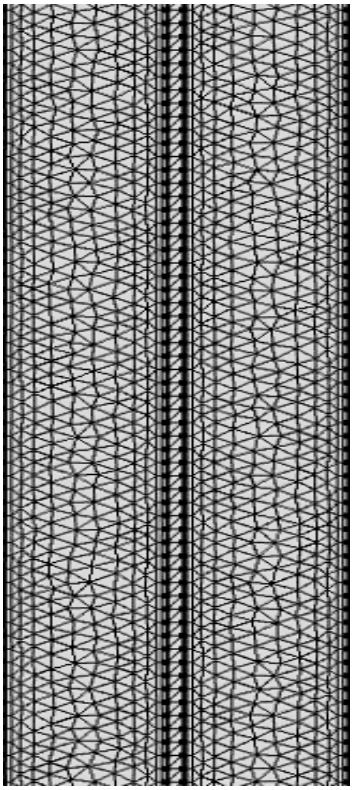

Figure 55: Fine Mesh

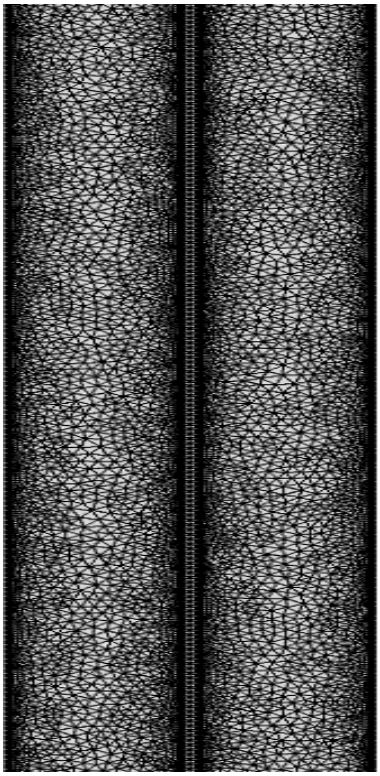

Figure 56:Extra Fine Mesh

4.3.3.1 Table

The values used in the table are as under:

Bulk feed temperature=333K

Bulk permeate temperature= 293K,

Bulk feed velocity = 0.5m/s

Bulk permeate velocity = 0.5m/s

Table 13: Flux comparison in COMSOL and MATLAB for different mesh qualities

Software	No of domain elements	No of boundary elements	Membrane Feed temperature (T_{mf}) (K)	Membrane permeate temperature (T_{mp}) (K)	Flux (COMSOL) (J) kg/m^2.hr	Flux (MATLAB) (J) kg/m^2.hr
Coarse	69394	8202	318.87	306.1	1.44	1.59
Fine	150834	13162	319.53	306.07	1.54	
Extra Fine	565615	28396	319.66	306.07	1.56	

4.3.3.2 Graph

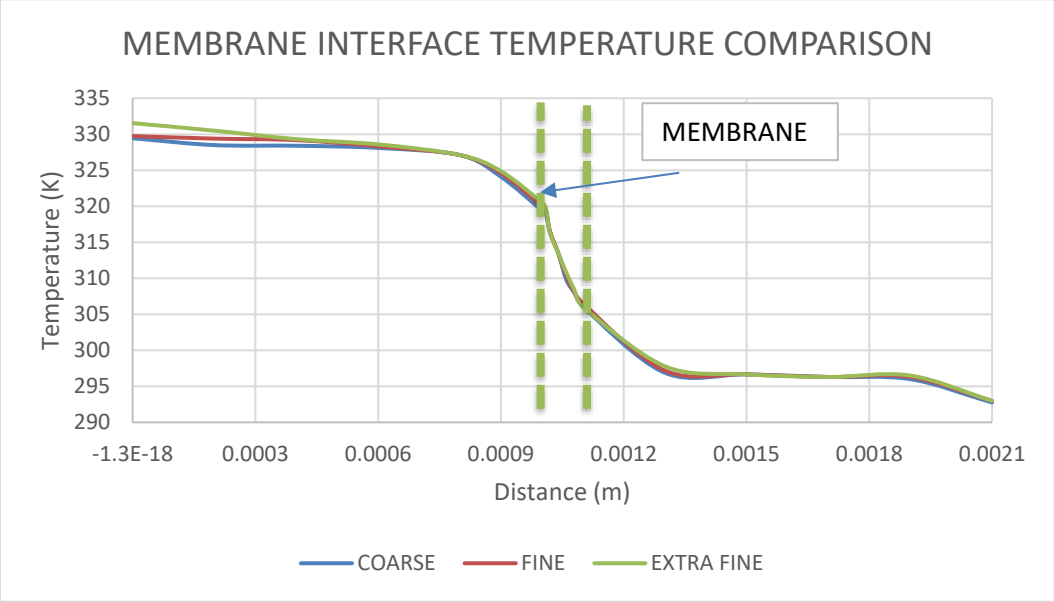

Figure 58: Comparison of Membrane Interface Temperatures at different Mesh qualities from COMSOL

4.3.3.2.1 Comment

We can see from the table and graph that as the mesh quality is increased, the system is divided into more elements and results come closer to actual value from research paper on the basis of which the matlab code has been designed. This verifies our results. We could have increased the quality of mesh refinement more but the processing power of our CPU limits this further grid advancement [62].

4.4 EXPERIMENTAL RESULTS

We carried out the different experimental results at different feed temperature for one hour.

Feed velocity = 0.5m/s

Permeate temperature = 293K

Table 14: Experimental results

Sr.No	Feed temperature (K)	Exp. Flux recorded ($kg/m^2.hr$)	Theo. Results from calculations ($kg/m^2.hr$)	TDS exp. (ppt)	TDS theo. (ppt)	Difference in flux
1	323	0.91	1.24	225	182	0.33
2	333	1.08	1.59	226	182	0.51
3	343	1.26	1.85	225	182	0.59

The difference between the values is due to the fact that theoretical analysis is being done on the basis of 100% removal of salts but in actual, our hydrophobic membrane is able to remove around 85-89% salts only, thus showing deviation in results.

4.4.1 Comparison of Experimental vs. Theorotical results

The following bar chart shows the comparison between experimental vest theoretical results

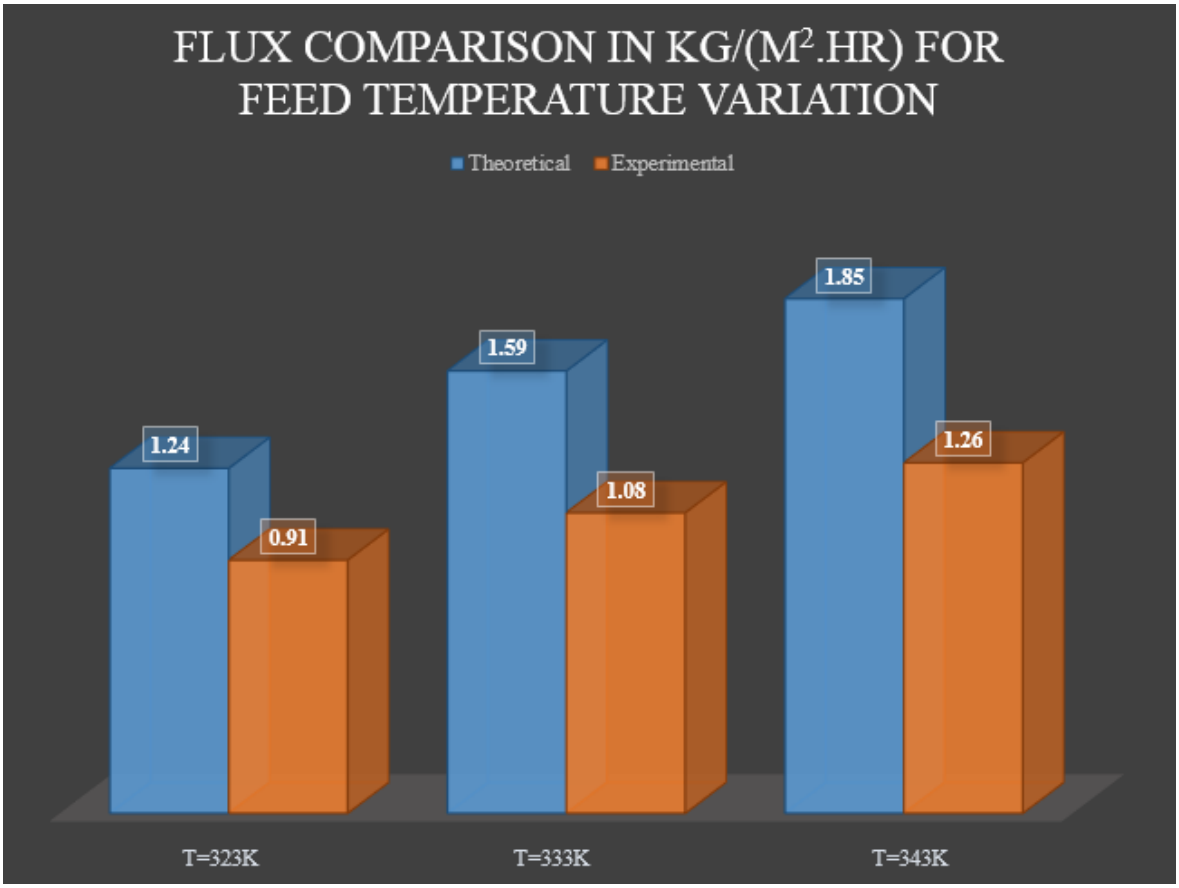

Figure 59: Experimental vs Theorotical results

CHAPTER 5: CONCLUSION AND RECOMMENDATION

5.1 Conclusions

A theoretical study of a solar powered DCMD module was presented. The parameters influencing the behavior of the system were studied theoretically and the results were compared with the literature. The analytical study was done by developing a mathematical model for the system based on mass and heat transfer inside the DCMD system. The mathematical model was solved using an iterative scheme with the help of MATLAB® software. These results were verified with a finite element analysis of the membrane module using COMSOL®. The performance trends obtained were compared with the literature. Based on the results, we drew the following conclusions:

- Membrane distillation is dependent on the temperature of water as increase of water vapor pressure occurs as temperature is enhanced. So increasing the feed water temperature caused exponential rise in permeate flux.
- Since permeate water is used for condensation in our system, therefore higher temperature of permeate water results in lesser membrane flux due to low temperature difference between the hot and cold fluids during condensation. This causes low condenser efficiency which lessens the water productivity.
- Increasing the porosity of the membrane results in a higher membrane flux.
- Conduction losses in the membrane module can be lowered down by using a thicker membrane, but this results in lower mass transfer. Therefore a tradeoff is required between the two parameters.
- The accuracy of the simulation results achieved by COMSOL® increases by increasing the quality of mesh used to discretize the membrane module. However this will require higher processing power and time. So a compromise must be made between accuracy and processing time.

5.2 Recommendations

Solar powered membrane distillation is suitable source to provide pure water in isolated areas where there is an abundance of solar irradiation. Since membrane distillation requires low operating temperature as compared to some other distillation technologies, it can easily be integrated with solar energy which has abundant resources. For future work, following points are recommended:

- To increase feed water temperature, higher absorber plate temperature in solar collector must be achieved. This can be done by using a parabolic trough.
- Although fouling and wetting of membranes are less problematic in membrane distillation as compared to reverse osmosis, more research is required to find out the exact causes and solutions to these parameters because they limit the performance and increase the associated cost of a MD process.
- To make solar powered membrane distillation more feasible, further research is required to improve the thermal efficiency and the performance of the system. This can be done by making better membranes and improving the design of the overall modules.
- Currently membrane distillation is being used primarily for the treatment of brackish or sea water. It can be used for waste water treatment with some modifications for which further study is required.

Our world is currently suffering from energy crisis and shortage of water. In the face of these circumstances, water distillation technologies driven by renewable energy resources like solar power are sustainable alternatives to these energy and water crisis. Solar energy resources are present in abundance and it will also decrease the harmful effects of traditional energy consumption on the environment. With further research and proper development of membrane and solar technologies, solar powered membrane distillation could become a valid course of action for future distillation plants.

REFERENCES

[1] Various water pollution facts (2016). Retrieved from: https://www.conserve-energy-future.com/various-water-pollution-facts.php

[2] 6 reasons why we need clean water for all (2015). Retrieved from: https://www.weforum.org/agenda/2015/09/6-reasons-why-we-need-clean-water-for-all

[3] How much water on earth (2010). Retrieved from: https://www.livescience.com/29673-how-much-water-on-earth.html

[4] Carvalho, G. A., Minnett, P. J., Fleming, L. E., Banzon, V. F., & Baringer, W. (2010). Satellite remote sensing of harmful algal blooms: A new multi-algorithm method for detecting the Florida Red Tide (Karenia brevis). *Harmful algae*, *9*(5), 440-448.

[5] Thomas, N., Mavukkandy, M. O., Loutatidou, S., & Arafat, H. A. (2017). Membrane distillation research & implementation: Lessons from the past five decades. *Separation and Purification Technology*, *189*, 108-127.

[6] Onsekizoglu, P. (2012). Membrane distillation: principle, advances, limitations and future prospects in food industry. In *Distillation-Advances from Modeling to Applications*. InTech.

[7] Susanto, H. (2011). Towards practical implementations of membrane distillation. *Chemical Engineering and Processing: Process Intensification*, *50*(2), 139-150.

[8] Al-Obaidani, S., Curcio, E., Macedonio, F., Di Profio, G., Al-Hinai, H., & Drioli, E. (2008). Potential of membrane distillation in seawater desalination: thermal efficiency, sensitivity study and cost estimation. *Journal of Membrane Science*, *323*(1), 85-98.

[9] Li, L., & Sirkar, K. K. (2017). Studies in vacuum membrane distillation with flat membranes. *Journal of Membrane Science, 523*, 225-234.

[10] Drioli, E., Ali, A., & Macedonio, F. (2015). Membrane distillation: recent developments and perspectives. *Desalination*, *356*, 56-84.

[11] Daer, S., Kharraz, J., Giwa, A., & Hasan, S. W. (2015). Recent applications of nanomaterials in water desalination: a critical review and future opportunities. *Desalination*, *367*, 37-48.

[12] Nicolaï, A., Sumpter, B. G., & Meunier, V. (2014). Tunable water desalination across graphene oxide framework membranes. *Physical Chemistry Chemical Physics*, *16*(18), 8646-8654.

[13] Alklaibi, A. M. (2008). The potential of membrane distillation as a stand-alone desalination process. *Desalination*, *223*(1-3), 375-385.

[14] Qtaishat, M., Matsuura, T., Kruczek, B., & Khayet, M. (2008). Heat and mass transfer analysis in direct contact membrane distillation. *Desalination*, *219*(1-3), 272-292.

[15] Cai, J., & Guo, F. (2017). Study of mass transfer coefficient in membrane desalination. *Desalination*, *407*, 46-51.

[16] Phattaranawik, J., & Jiraratananon, R. (2001). Direct contact membrane distillation: effect of mass transfer on heat transfer. *Journal of Membrane Science*, *188*(1), 137-143.

[17] Bodell, B. R. (1968). *U.S. Patent No. 3,361,645*. Washington, DC: U.S. Patent and Trademark Office.

[18] Lee, J. G., & Kim, W. S. (2013). Numerical modeling of the vacuum membrane distillation process. *Desalination*, *331*, 46-55.

[19] Mengual, J. I., Khayet, M., & Godino, M. P. (2004). Heat and mass transfer in vacuum membrane distillation. *International Journal of Heat and Mass Transfer*, *47*(4), 865-875.

[20] Khalifa, A., Lawal, D., Antar, M., & Khayet, M. (2015). Experimental and theoretical investigation on water desalination using air gap membrane distillation. *Desalination*, *376*, 94-108.

[21] Khalifa, A. E., Alawad, S. M., & Antar, M. A. (2017). Parallel and series multistage air gap membrane distillation. *Desalination*, *417*, 69-76.

[22] García-Fernández, L., Wang, B., García-Payo, M. C., Li, K., & Khayet, M. (2017). Morphological design of alumina hollow fiber membranes for desalination by air gap membrane distillation. *Desalination*, *420*, 226-240.

[23] Khayet, M., Godino, M. P., & Mengual, J. I. (2003). Theoretical and experimental studies on desalination using the sweeping gas membrane distillation method. *Desalination*, *157*(1-3), 297-305.

[24] Khayet, M., Cojocaru, C., & Baroudi, A. (2012). Modeling and optimization of sweeping gas membrane distillation. *Desalination*, *287*, 159-166.

[25] Karanikola, V., Corral, A. F., Jiang, H., Sáez, A. E., Ela, W. P., & Arnold, R. G. (2015). Sweeping gas membrane distillation: numerical simulation of mass and heat transfer in a hollow fiber membrane module. *Journal of Membrane Science*, *483*, 15-24.

[26] González, D., Amigo, J., & Suárez, F. (2017). Membrane distillation: Perspectives for sustainable and improved desalination. *Renewable and Sustainable Energy Reviews*, *80*, 238-259.

[27] Ali, A., Tufa, R. A., Macedonio, F., Curcio, E., & Drioli, E. (2018). Membrane technology in renewable-energy-driven desalination. *Renewable and Sustainable Energy Reviews*, *81*, 1-21.

[28] Banat, F., Jumah, R., & Garaibeh, M. (2002). Exploitation of solar energy collected by solar stills for desalination by membrane distillation. *Renewable Energy*, *25*(2), 293-305.

[29] Nakoa, K., Rahaoui, K., Date, A., & Akbarzadeh, A. (2015). An experimental review on coupling of solar pond with membrane distillation. *Solar Energy*, *119*, 319-331.

[30] Banat, F., & Jwaied, N. (2008). Exergy analysis of desalination by solar-powered membrane distillation units. *Desalination*, *230*(1-3), 27-40.

[31] Qiblawey, H. M., & Banat, F. (2008). Solar thermal desalination technologies. *Desalination*, *220*(1-3), 633-644.

[32] Schwantes, R., Cipollina, A., Gross, F., Koschikowski, J., Pfeifle, D., Rolletschek, M., & Subiela, V. (2013). Membrane distillation: Solar and waste heat driven demonstration plants for desalination. *Desalination*, *323*, 93-106.

[33] Chang, H., Lyu, S. G., Tsai, C. M., Chen, Y. H., Cheng, T. W., & Chou, Y. H. (2012). Experimental and simulation study of a solar thermal driven membrane distillation desalination process. *Desalination*, *286*, 400-411.

[34] Wang, X., Zhang, L., Yang, H., & Chen, H. (2009). Feasibility research of potable water production via solar-heated hollow fiber membrane distillation system. *Desalination*, *247*(1-3), 403-411.

[35] Mericq, J. P., Laborie, S., & Cabassud, C. (2011). Evaluation of systems coupling vacuum membrane distillation and solar energy for seawater desalination. *Chemical Engineering Journal*, *166*(2), 596-606.

[36] Zhang, Y., Sivakumar, M., Yang, S., Enever, K., & Ramezanianpour, M. (2018). Application of solar energy in water treatment processes: A review. *Desalination*, *428*, 116-145.

[37] Pouyfaucon, A. B., & García-Rodríguez, L. (2018). Solar thermal-powered desalination: A viable solution for a potential market. *Desalination*.

[38] Li, C., Goswami, Y., & Stefanakos, E. (2013). Solar assisted sea water desalination: A review. *Renewable and Sustainable Energy Reviews*, *19*, 136-163.

[39] Kabeel, A. E., Abdelgaied, M., & El-Said, E. M. (2017). Study of a solar-driven membrane distillation system: Evaporative cooling effect on performance enhancement. *Renewable Energy*, *106*, 192-200.

[40] Suárez, F., Ruskowitz, J. A., Tyler, S. W., & Childress, A. E. (2015). Renewable water: direct contact membrane distillation coupled with solar ponds. *Applied energy*, *158*, 532-539.

[41] Duong, H. C., Xia, L., Ma, Z., Cooper, P., Ela, W., & Nghiem, L. D. (2017). Assessing the performance of solar thermal driven membrane distillation for seawater desalination by computer simulation. *Journal of Membrane Science*, *542*, 133-142.

[42] Chang, H., Wang, G. B., Chen, Y. H., Li, C. C., & Chang, C. L. (2010). Modeling and optimization of a solar driven membrane distillation desalination system. *Renewable energy*, *35*(12), 2714-2722.

[43] Chafidz, A., Kerme, E. D., Wazeer, I., Khalid, Y., Ajbar, A., & Al-Zahrani, S. M. (2016). Design and fabrication of a portable and hybrid solar-powered membrane distillation system. *Journal of cleaner production*, *133*, 631-647.

[44] Fath, H. E., & Ghazy, A. (2002). Solar desalination using humidification—dehumidification technology. *Desalination*, *142*(2), 119-133.

[45] Midilli, A., & Ayhan, T. (2004). Natural vacuum distillation technique—part I: theory and basics. *International journal of energy research*, *28*(4), 355-371.

[46] González, D., Amigo, J., & Suárez, F. (2017). Membrane distillation: Perspectives for sustainable and improved desalination. *Renewable and Sustainable Energy Reviews*, *80*, 238-259.

[47] Shukla, A., Kant, K., & Sharma, A. (2017). Solar still with latent heat energy storage: A review. *Innovative Food Science & Emerging Technologies*, *41*, 34-46.

[48] Rahaoui, K., Ding, L. C., Tan, L. P., Mediouri, W., Mahmoudi, F., Nakoa, K., & Akbarzadeh, A. (2017). Sustainable Membrane Distillation Coupled with Solar Pond. *Energy Procedia*, *110*, 414-419

[49] Hasanizadeh, M., Jafari, P., Farshighazani, B., & Moraveji, M. K. (2016). CFD simulation of heat and mass transport for water transfer through hydrophilic membrane in direct-contact membrane distillation process. *Desalination and Water Treatment*, *57*(39), 18109-18119.

[50] Soukane, S., Naceur, M. W., Francis, L., Alsaadi, A., & Ghaffour, N. (2017). Effect of feed flow pattern on the distribution of permeate fluxes in desalination by direct contact membrane distillation. *Desalination*, *418*, 43-59.

[51] Yu, H., Yang, X., Wang, R., & Fane, A. G. (2012). Analysis of heat and mass transfer by CFD for performance enhancement in direct contact membrane distillation. *Journal of membrane science, 405*, 38-47.

[52] Hayer, H., Bakhtiari, O., & Mohammadi, T. (2015). Analysis of heat and mass transfer in vacuum membrane distillation for water desalination using computational fluid dynamics (CFD). *Desalination and Water Treatment*, *55*(1), 39-52.

[53] Tijing, L. D., Woo, Y. C., Choi, J. S., Lee, S., Kim, S. H., & Shon, H. K. (2015). Fouling and its control in membrane distillation—a review. *Journal of Membrane Science*, *475*, 215-244.

[54] Cipollina, A., Di Sparti, M. G., Tamburini, A., & Micale, G. (2012). Development of a membrane distillation module for solar energy seawater desalination. *Chemical engineering research and design*, *90*(12), 2101-2121.

[55] Schofield, R. W., Fane, A. G., & Fell, C. J. D. (1987). Heat and mass transfer in membrane distillation. *Journal of Membrane Science*, *33*(3), 299-313.

[56] Lawal, D. U., & Khalifa, A. E. (2014). Flux prediction in direct contact membrane distillation. *Int. J. Mater. Mech. Manuf*, *2*(4), 302-308

[57] Nakoa, K., Date, A., & Akbarzadeh, A. (2016). DCMD modelling and experimental study using PTFE membrane. *Desalination and Water Treatment*, *57*(9), 3835-3845.

[58] Laganà, F., Barbieri, G., & Drioli, E. (2000). Direct contact membrane distillation: modelling and concentration experiments. *Journal of Membrane Science*, *166*(1), 1-11.

[59] Smolders, K. F. A. C. M., & Franken, A. C. M. (1989). Terminology for membrane distillation. *Desalination*, *72*(3), 249-262.

[60] Duffie, J. A., & Beckman, W. A. (2013). Solar engineering of thermal processes. John Wiley & Sons

[61] Saleh, A. M. (2012). *Modeling of flat-plate solar collector operation in transient states* (Doctoral dissertation, Purdue University).

[62] Ghadiri, M., Fakhri, S., & Shirazian, S. (2014). Modeling of water transport through nanopores of membranes in direct-contact membrane distillation process. *Polymer Engineering & Science*, *54*(3), 660-666.

[63] Hwang, H. J., He, K., Gray, S., Zhang, J., & Moon, I. S. (2011). Direct contact membrane distillation (DCMD): Experimental study on the commercial PTFE membrane and modeling. *Journal of Membrane Science*, *371*(1-2), 90-98.

[64] Pranit M. Patil, Amol P. Yadav, Dr. P. A. Patil. "Comparative Study between Heat Transfer through Laminar Flow and Turbulent Flow".

[65] Hwang, S. T., & Kammermeyer, K. (1974). Effect of thickness on permeability. In *Permeability of Plastic Films and Coatings* (pp. 197-205). Springer, Boston, MA.

[66] Adnan, S., Hayat Khan, A., Haider, S., & Mahmood, R. (2012). Solar energy potential in Pakistan. *Journal of Renewable and Sustainable Energy*, *4*(3), 032701.